

Research Article

Title: The olfactory pathway of the hornet *Vespa velutina*: new insights into the evolution of the hymenopteran antennal lobe

Authors: Antoine Couto ¹, Benoit Lapeyre ¹, Denis Thiéry ^{2,3}, and Jean-Christophe Sandoz ^{1,*}

Institutional affiliations:

¹ Laboratory Evolution Genome Behavior and Ecology, CNRS, Univ Paris-Sud, IRD, Université Paris Saclay, 1 avenue de la Terrasse, F-91198 Gif-sur-Yvette, France

² UMR 1065 Santé et Agroécologie du Vignoble, INRA, F-33883 Villenave d'Ornon, France

³ Université de Bordeaux, ISVV, UMR 1065 Santé et Agroécologie du Vignoble, Bordeaux Sciences Agro, F-33883 Villenave d'Ornon, France

Key words: social insect, wasps, three-dimensional reconstruction, macroglomerulus, RRID:SCR_000450, RRID:SCR_003070, RRID:SCR_007353, RRID:SCR_013672

*: Corresponding author: J.C. Sandoz

e-mail: sandoz@egce.cnrs-gif.fr

phone: +33 1 69 82 37 51

fax: +33 1 69 82 37 36

Grant sponsor: This work was supported by a grant from Région Ile-de-France to J.C.S. (DIM R2DS, project 2011-05).

This article has been accepted for publication and undergone full peer review but has not been through the copyediting, typesetting, pagination and proofreading process which may lead to differences between this version and the Version of Record. Please cite this article as an 'Accepted Article', doi: 10.1002/cne.23975

© 2016 Wiley Periodicals, Inc.

Received: Nov 20, 2015; Revised: Jan 20, 2016; Accepted: Jan 29, 2016

Abstract

In the course of evolution, eusociality has appeared several times independently in Hymenoptera, within different families such as Apidae (bees), Formicidae (ants) and Vespidae (wasps and hornets) among others. The complex social organization of eusocial Hymenoptera relies on sophisticated olfactory communication systems. While the olfactory systems of several bee and ant species have been well characterized, very little information is yet available in Vespidae, although this family represents a highly successful insect group, displaying a wide range of lifestyles from solitary to eusocial. Using fluorescent labeling, confocal microscopy and 3D reconstructions, we investigated the organization of the olfactory pathway in queens, workers and males of the eusocial hornet *Vespa velutina*. First, we found that caste and sex dimorphism is weakly pronounced in hornets, both with regards to whole brain morphology and antennal lobe organization, although several male-specific macroglomeruli are present. The *Vespa velutina* antennal lobe contains about 265 glomeruli (in females), grouped in 9 conspicuous clusters formed by afferent tract subdivisions. As in bees and ants, hornets display a dual olfactory pathway, with two major efferent tracts, the medial and the lateral antennal lobe tracts (m- and l-ALT), separately arborizing two antennal lobe hemilobes and projecting to partly different regions of higher-order olfactory centers. Lastly, we found remarkable anatomical similarities between the glomerular cluster organizations of hornets, ants and bees, suggesting the possible existence of homologies in the olfactory pathways of these eusocial Hymenoptera. We propose a common framework for describing AL compartmentalization across Hymenoptera and discuss possible evolutionary scenarios.

Introduction

Insects are influential models in the study of the evolution of olfactory processing and have revealed how selection pressures influence the organization and complexity of the olfactory system (Rospars, 1988; Kleineidam and Rössler, 2009; Ramdya and Benton, 2010; Hansson and Stensmyr, 2011). In insects, volatile molecules are detected by olfactory sensory neurons (OSNs) housed in cuticular sensilla on the antennae (Zacharuk, 1980). These neurons project to a primary olfactory center, the antennal lobe (AL), where they synapse onto local interneurons and projection neurons (PNs), within dense synaptic neuropils, the glomeruli (Hildebrand and Shepherd, 1997; Anton and Homberg, 1999; Vosshall et al., 2000). PNs convey the olfactory message processed within AL networks to higher-order olfactory centers, the mushroom body (MB) and/or the lateral horn (LH).

Many previous works have revealed specific adaptations in AL organization, in relation with the particular biology and ecology of a wide range of insect species (Rospars, 1983; Martin et al., 2011; Clifford and Riffell, 2013). For instance, while the number of AL glomeruli is almost invariant among individuals of a given species, it varies greatly between species, which is thought to be related to the complexity of their olfactory environments (Anton and Homberg, 1999; Hansson and Anton, 2000; Kelber et al., 2009). Another striking example of such neuroanatomical and physiological adaptations is the existence of enlarged glomeruli, called macroglomeruli, dedicated to pheromone detection and processing (Burrows et al., 1982; Arnold et al., 1985; Hanson et al., 1992; Sandoz, 2006; Nishikawa et al., 2008; Nishino et al., 2012). In most cases, macroglomeruli are male dimorphic adaptations devoted to sex pheromone processing, but they have also been discovered in the females of some social Hymenoptera (Arnold et al., 1988; Kleineidam et al., 2005; Roselino et al., 2015). In leaf cutting ants, for instance, a macroglomerulus found only in large workers is thought to process trail pheromone information (Kelber et al., 2009; Kuebler et al., 2010). Thus, the

presence of hypertrophied glomeruli may inform about particular pheromonal communication channels in a species. In some cases, neuronal adaptations of the olfactory pathway are found throughout a specific taxon. For instance, in Hymenoptera, uniglomerular PNs project to the MB and the LH through two parallel output tracts, the medial and the lateral antennal lobe tracts (m- and l-ALT). The AL is thus composed of two hemilobes which send their information separately to both higher-order centers (Abel et al., 2001; Galizia and Rössler, 2010; Rössler and Zube, 2011; Rössler and Brill, 2013). Investigations in basal Hymenoptera showed that this neuronal organization is present in some sawfly (Symphyta) families but absent in others, leading to the hypothesis that it has evolved in basal Hymenoptera (Dacks and Nighorn, 2011; Rössler and Zube 2011). The benefit of this parallel processing system and the selective pressures that favored its evolution still remain unknown. Some authors hypothesized that it could represent a pre-adaptation to high demands on olfactory discrimination needed for particular life styles like parasitism, central place foraging or sociality (Galizia and Rössler, 2010; Rössler and Zube, 2011). The above examples demonstrate that essential knowledge on the evolution of the insect olfactory system can be obtained from its comparative analysis in well-chosen taxa. Thus, comparing the organization of the AL, and its specific adaptations in terms of glomerular number, size and input-output connectivity may allow one to understand adaptations linked to changes in diet, host preference or social lifestyle in Hymenoptera (Rosspars, 1983; Zube and Rössler, 2008; Kelber et al., 2009; Dacks et al., 2010; Ibba et al., 2010; Guidobaldi et al., 2014; Das and Fadamiro, 2013).

Social insects ensure colony defense and cohesion, division of labor and behavioral regulation through a highly elaborate communication system (Vander Meer, 1998). Specific adaptations of the olfactory pathway can be observed among the different members of an eusocial insect colony, which are usually revealed through sex- and caste- polymorphism

(Zube and Rössler, 2008; Groh and Rössler, 2008; Kuebler et al., 2010; Nakanishi et al., 2010; Stieb et al., 2011; Roselino et al., 2015). Interestingly, eusociality has appeared several times in Hymenoptera, in at least three different families, Apidae (bees), Formicidae (ants) and Vespidae (wasps and hornets) (Hines et al., 2007; Hughes et al., 2008; Cardinal and Danforth, 2011; Johnson et al.; 2013). While possible adaptations of olfactory circuits related to the social lifestyle have been investigated in several Apidae (honey bees, stingless bees : Arnold et al., 1985; Flanagan and Mercer, 1989; Galizia et al., 1999; Kelber et al., 2006; Nishino et al., 2009; Streinzer et al., 2013; Roselino et al., 2015) and Formicidae (several ant species: Nishikawa et al., 2008; Zube and Rössler, 2008; Mysore et al., 2009; Nakanishi et al., 2010; Stieb et al., 2011; Kuebler et al., 2010), Vespidae are poorly documented. This group represents however a key group for studying the evolution of eusociality because they present a wide range of social organizations, from solitary to eusocial (Hunt, 2007; Pickett and Carpenter, 2010). In their highest level of sociality, Vespidae display a large repertoire of odor-guided behaviors comparable to those of ants and bees, including kin recognition and cooperation for brood care, colony defense and foraging (Spradbery, 1973; Edwards 1980; Matsuura and Yamane, 1990; Oi et al., 2015). Hornets (*Vespa* sp.) are the largest sized eusocial wasps. They are generalist foragers which gather carbohydrates and proteins for their progeny, by exploiting flower nectar, tree sap, fruit pulp and arthropod preys (Raver et Richter, 2000). For such task, they use odors emanating from the food sources but also intraspecific olfactory recruitment signals, which increase their foraging efficiency (Ono et al., 1995; Ono et al., 2003; Brodmann et al., 2009; Couto et al., 2014). Females can release scent marks which are used by both workers and males to locate the nest (Batra, 1980; Steinmetz et al., 2002; Tan, 2014). Within the nest, hornets live in organized colonies with a highly efficient task allocation system regulated through social pheromones acting on workers (Ikan et al., 1969; Ishay, 1973; Veith et al., 1984; Monceau et al., 2013). To prevent

exploitation of such altruistic behavior by alien individuals, hornets are also able to discriminate nestmates and non-nestmates by means of cuticular hydrocarbons (Ruther et al., 1998; Ruther et al., 2002). In addition, queens produce a sex pheromone that triggers copulatory behavior in males (Batra, 1980; Ono and Sasaki, 1987; Spiewok et al., 2006). Therefore, both hornet males and females develop and live in a rich olfactory environment and use a wide range of inter- and intraspecific chemical cues (Bruchini et al., 2010).

To date very few works have described the central nervous system of Vespidae, and most studies date back to more than a century (Flögel, 1878; Viallanes, 1887; von Alten, 1910). Flögel (1878) proposed the first anatomical description of the wasp brain and observed striking differences in the morphology of its MBs compared to the brains of other eusocial Hymenoptera, such as ants and honey bees. This was confirmed by Viallanes (1887) who reported that despite the huge size of their MBs, the vertical (α) and medial (β) lobes appear atrophied. More recently, Ehmer and Hoy (2000) highlighted a strong anatomical divergence of MBs within this family, which could however not be related with the social organization level of the investigated species. Since then, neuroanatomical studies on the wasp or hornet brain mainly focused on higher-order centers (O'Donnell et al., 2004, 2011, 2015), but its olfactory pathway, and especially the AL, which may support important adaptations for foraging, pheromonal processing and/or sociality, has been the subject of little consideration. According to Hanström (1928), the AL of social wasps would contain ~1000 small glomeruli arranged in multiglomerular layers, as in locusts (Hansson and Anton 2000). In theory, such a high number of glomeruli would be consistent with the rich olfactory environment of these species. However, in the light of recent data, serious doubts can be emitted concerning Hanström's (1928) description (Kelber et al., 2009). First, none of the so-far studied Hymenoptera displays such a high number of glomeruli, the maximum being 630 glomeruli in the ant *Apterostigma cf. mayri* (Kelber et al., 2009). Second, given current knowledge on the

neural organization of the olfactory pathways of the different insect orders, it seems highly unlikely that the hornet AL presents a true locust-like organization, especially with regard to PNs arborization. While PNs are multiglomerular in locusts (Ignell, 2001; Ignell et al., 2001; Anton et al., 2002), Hymenoptera typically display two major tracts of uniglomerular PNs, and three lesser tracts of multiglomerular PNs which form a broad network in the protocerebrum (medio-lateral ALT, ml-ALT; Abel et al., 2001; Kirschner et al., 2006; Galizia and Rössler, 2010; Rössler and Zube, 2011).

In the present study we performed a detailed neuroanatomical exploration of the olfactory pathway of a eusocial Vespidae, the hornet *Vespa velutina*. This otherwise typical hornet species is particularly remarkable for its ecological success when introduced to new locations, as for instance in Europe, in which it has become an invasive species (Monceau et al., 2014; Arca et al., 2015). A nest founded by a single mated queen can produce up to 13,000 individuals, mostly sterile females (workers), which actively cooperate for the survival of the colony (Rome et al., 2015). They are vigorous predators of insects and very actively prey on honey bees, representing a threat for both local biodiversity and beekeeping activities (Monceau et al., 2014). Using fluorescent dye injection coupled with confocal microscopy, we compared AL features in queens, workers and males. We asked whether the hornet olfactory system displays caste- or sex-specific adaptations, potentially related to the roles of the different members of a hornet colony. In particular, we looked for differences in the organization, size and volume of AL glomeruli. Furthermore, in an evolutionary perspective, we investigated the input-output connectivity of the AL, and compared it to the well-described olfactory pathways of ants and honeybees.

Materials and Methods

1. Animals

Queens, workers and males of the yellow-legged hornet, *Vespa velutina*, were used in the experiments. Queens and workers were obtained from field trapping in the area of INRA-Bordeaux Aquitaine (France) between April and November. Males were collected from wild nests in September in the same area. Males were identified thanks to their specific morphological features such as long antennae (11 antennal segments instead of 10 in females) and the lack of a sting. Females were assigned to the reproductive or sterile caste by measuring their wing area according to Perrard et al (2012). Wings were carefully flattened and clamped between 2 glass slides before capturing images with a film scanner (OpticFilm 7400, Plustek, Taipei, Taiwan). Wing size was evaluated using ImageJ (RRID:SCR_003070). A proxy measure of wing size was defined as the area between 9 conspicuous vein intersections of the forewing (Fig. 1A, corresponding to landmarks 1, 2, 3, 4, 9, 10, 13, 15 and 16 in Perrard et al., 2012). In hornets, queens are usually larger than workers (Matsuura and Yamane, 1990). However, in *V. velutina*, this difference is not so clear cut as in other species (Perrard et al., 2012). In particular, due to an increase in the size of emerging workers in the course of colony cycle, wing areas of the two female castes may overlap in autumn, whereas they are clearly different in early summer. Therefore, females captured from April to June with a large wing area could be unambiguously assigned to queens while small females captured from July to November could likewise be assigned to workers (Fig. 1B). Only such clearly identifiable individuals were used in this study (Fig. 1B; dark grey: workers; light grey: queens). For all experiments, hornets were anesthetized on crushed ice for 10 min before placing them into individual Plexiglas holders (see Sandoz et al., 2003, Fig. 1).

2. Neuroanatomical staining

2.1 Whole brain neuropil staining

To visualize and reconstruct the hornet brain, Lucifer yellow was used as a neuropil background stain (Ai and Kanzaki, 2004; Rybak et al., 2010). The head of each hornet was fixed to the chamber with low melting point wax (Deiberit 502, Schöps and Dr Böhme, Goslar, Germany) and the head capsule was opened. The brain was dissected out under phosphate buffered saline (PBS) solution. It was then immediately transferred to 500 μ L of fixative solution (4% paraformaldehyde in PBS) containing 1 μ L of 4% Lucifer yellow (Lucifer Yellow CH, Potassium Salt, L-1177; Invitrogen, Eugene, OR) and kept for 4 days at 4°C.

2.2 Specific neuronal staining

To describe the glomerular organization of the antennal lobe, antennal sensory neurons were stained anterogradely. A window was cut into the scape of each antenna and the antennal nerves were severed with a glass electrode loaded with crystals of fluoro-ruby (Tetramethylrhodamine dextran, 10 000 MW, D-1817; Invitrogen, Eugene, OR; in 2% Bovine Serum Albumin). The preparation was then covered with saline solution (130 mM NaCl, 6 mM KCl, 4 mM MgCl₂, 5 mM CaCl₂, 160 mM sucrose, 25 mM glucose, 10 mM HEPES, with PH = 6.7) and kept 24 hours in a dark room to let the dye diffuse. The next day, the brain was dissected out and plunged into 4% PFA solution for 24 hours at 4°C.

For visualization of projections of antennal lobe tracts (ALTs) through the protocebrum towards higher order centers, a massive dye injection in the AL was performed. The hornet's head cuticle was removed by cutting a rectangle between the antenna and the compound eyes to expose the AL neuropil. Subsequently, a glass electrode coated with fluoro-ruby was

inserted into the AL and kept in this position until dissolution of the dye crystal, allowing uptake by injured AL neurons, including projection neurons (PNs). The electrode was then dislodged from the AL, and the brain was washed with saline solution to remove extra dye. As above, preparations were kept 24 hours in a dark room during dye migration before brains were dissected out and fixated in 4% PFA.

2.3 Double labeling

To assign AL glomeruli to one of the two main PN tracts (l-ALT, m-ALT or both) each tract was retrogradely labeled with different dyes in the same preparation. A piece of head cuticle was removed to expose the region between the ALs and the mushroom body calyces. The l-ALT was labeled by fluorescent tracer injection (Dextran, Alexa Fluor 488, 10 000 MW, D-22910; Invitrogen, Eugene, OR; in 2% BSA) into the caudo-lateral area of the protocerebrum where the l-ALT runs between the AL and the lateral horn. The m-ALT was labeled by fluoro-ruby injection into the medio-caudal area of the protocerebrum, where the m-ALT runs between the AL and the MB. To avoid unspecific staining, extra dye was removed after each injection by washing the brain with saline solution. After 24 hours of dye migration, the brains were dissected out and fixated in 4% PFA.

To visualize olfactory and visual inputs to the MB calyces, AL projection neurons and visual output neurons were separately stained in the same preparation by mass tracer injections of Alexa Fluor into the AL and fluoro-ruby into the optic lobe (medulla and lobula).

3. Brain preparations

After being removed from the fixative solution, all brains were washed 3 times in PBS solution (10 min each), dehydrated in ethanol baths following an ascending series (50, 70, 90,

95 and 3 x 100% for 10 min each) and clarified in methylsalicylate (Sigma-Aldrich, Steinheim, Germany) for at least 3 days at 4°C. Brains were then mounted on aluminum slides with a central hole filled with methylsalicylate and covered by thin coverslips on both sides.

4. Confocal microscopy

Clarified brains were scanned from the ventral side with a laser-scanning confocal microscope (LSM-700; Carl Zeiss, Jena, Germany). Whole brain optical sections were acquired at a resolution of 2.5 $\mu\text{m}/\text{pixels}$ (x,y) with 3 μm intervals (z) using a water immersion objective (10x achroplan 0.3 NA). Antennal lobe optical sections were acquired at 0.52 $\mu\text{m}/\text{pixels}$ (x,y) with 1 μm intervals (z) using a water immersion objective (20x plan-apochromat 1.0 NA). Given the large size of the hornet brain, complete scans were obtained by stitching adjacent “tiles” (512 x 512 pixels) of optical sections with the tile function of the ZEN software (Carl Zeiss, Jena, Germany; RRID:SCR_013672). Fluoro-ruby labeled neurons were visualized using a 555 nm solid-state laser, whereas Lucifer yellow and Alexa Fluor were visualized using a 488 nm laser. Doubly stained neuropils were scanned sequentially to avoid emission overlap from distinct fluorescent dyes.

5. 3D reconstructions and olfactory tract affiliation

Serial optical sections were saved as LSM files before adjusting brightness and contrast with ImageJ software and the Bio-formats plugin (RRID:SCR_000450). Adjusted pictures were then converted into TIFF files and imported into three-dimensional analysis software (AMIRA 5.4.3, FEI, Berlin, Germany; RRID:SCR_007353). Glomeruli were individually

270 reconstructed by manual labeling in three planes (xy , xz and yz) and using the *wrap* function to
271 obtain its 3D model. Larger structures, such as brain neuropils and macroglomeruli, were
272 outlined in several stacks along one focal plane (xy), and the *interpolate* function was used to
273 create the 3D model.

274 Each reconstructed glomerulus was assigned to a glomerular cluster by closely following
275 OSN bundles in the original scan. Since similar features such as input tract trajectories,
276 glomerular morphologies and output tract affiliations could be observed in different
277 hymenopteran species, we attempted to unify olfactory tract nomenclature. Within each
278 species, antennal sensory tracts had been previously named with numbers (T1-Tx), starting
279 from the ventral to the dorsal surface of the antennal lobe (*Apis mellifera*: Suzuki, 1975;
280 Flanagan and Mercer, 1989; Galizia et al., 1999; Kirschner et al., 2006; Nishino et al., 2009;
281 *Camponotus* sp.: Zube et al., 2008, Nakanishi et al., 2010, Mysore et al., 2009; *Atta*
282 *vollenweideri*: Kelber et al., 2009; *Cataglyphis* sp.: Stieb et al., 2011), resulting in a mismatch
283 in tract designations between presumably homologous ones. In the present study, we thus
284 used a novel nomenclature, naming glomerular clusters with Roman letters ($T_A - T_I$), starting
285 from the dorsal surface to the ventral surface, as this arrangement better revealed similarities
286 among different species. From the above listed species, the hornet antennal lobe was
287 especially compared with those of honeybees and carpenter ants because these species
288 provide solid data on AL input-output connectivity. For honeybees *Apis mellifera*, we used
289 the description of antennal lobe compartmentalization made by Kirschner et al. (2006),
290 Nishino et al. (2009) and our personal data. For carpenter ants, the descriptions by Zube et al.
291 (2008) and Zube and Rössler (2008) in *Camponotus floridanus* and Nakanishi et al. (2010) in
292 *C. japonicus* were used.

293 Spatial directions given in each figure are based on the neuraxis (Strausfeld, 2002, Fig. 1H
294 therein). Consequently, rostral and caudal correspond respectively to anterior and posterior,

according to the body axis. The “frontal” surface of the brain corresponds to its most ventral region in the neuraxis.

6. Data analysis and statistics

To assess caste dimorphism in the number of glomeruli, a Mann-Whitney U test was used on 6 reconstructed ALs from each hornet caste. Potential type I errors induced by multiple comparisons were reduced by using a Bonferroni correction ($\alpha_{\text{corr}} = 0.05/2 = 0.025$).

Glomerular volumes were calculated from 3D reconstructions using Amira 5.4.3. To identify macroglomeruli and overcome the problem of antennal lobe size variability in different individuals, the volume of each glomerulus was normalized with respect to the size of the respective antennal lobe (calculated as the sum of all glomerular volumes, Fig. 4D). Then, a quantitative threshold that defines outliers according to 80% of the distribution of glomerular volumes was used:

$$V_{\text{outlier}} > V_U + k (V_U - V_L)$$

Where V_U is the upper percentile (90%) and V_L is the lower percentile (10%) of glomerular volume distribution. We used $k = 3$ as a conservative value that successfully categorized macroglomeruli in several hymenopteran species (Kuebler et al., 2010; Streinzer et al., 2013; Roselino et al., 2015). Thus, glomeruli whose volume was above this threshold were considered as macroglomeruli.

Results

General brain morphology

Vespa velutina males and females can be distinguished based on head and abdomen morphology, whereas there are no evident morphological differences between the two female castes (worker and queen, Fig. 2). Queens (Fig. 2A) are usually larger than workers (Fig. 2C), but the sizes of these two castes may sometimes overlap because of the increase in the body dimensions of workers produced throughout the colony cycle. Males' heads (Fig. 2E) show a typical triangular shape that is more elongated than females', with slightly more bulbous compound eyes. In addition, males' antennae are longer than females', with shorter scapes but 11 flagellum segments instead of 10 in females. Confocal image stacks acquired from whole brain staining in each caste allowed 3D reconstruction of selected neuropils (Fig. 2B, D, F). No clear differences in brain structure were observed between sexes or between female castes, the different neuropils occupying similar relative volumes in all these individuals (Table 1). In particular, both male and female hornets display voluminous visual sensory structures, with 30.6 % of brain volume occupied by the medulla and the lobula in the queen, 32.3 % in the worker and 34.7 % in the male. Likewise, the primary olfactory centers, the antennal lobes (ALs) display only slight sexual differences in their relative sizes, with 7.2 % and 7.1 % of brain volume in queen and worker respectively, and 9.2 % in the male.

Hornets' mushroom bodies have a characteristic shape, with two highly voluminous calyces on each brain hemisphere, and comparatively small peduncle and lobes (Fig. 2B, D, F). Like in other Hymenoptera (bees, ants, etc.), the calyces are composed of 3 concentric and morphologically distinct areas: the collar, the lip and the basal ring. However, in each calyx, the lips are placed more centrally compared to the collar which bulges around the lip, resembling a double-lip from an external view point (Fig. 2B, D, F). Differential mass staining of optic lobe and AL revealed that the collars are targeted by visual outputs neurons,

whereas the lips receive only olfactory input (Fig. 3A, B). While our staining procedure revealed strong olfactory input in the hornet basal ring, we could observe only sparse visual input in this area. Although this differential staining was not aimed at detailing visual sensory projections in the hornet brain, it suggested a similar arrangement of these projections as in honey bees (Mobbs, 1984; Ehmer and Gronenberg, 2002; Mota et al., 2011). Shortly, a prominent visual tract, the anterior optic tract (AOT), projects into the anterior optic tubercle while in the rostral part of the brain a neuronal network composed of several subtracts connects the medulla and lobula with ipsi- and contralateral MB calyces. Direct inter-hemispheric connections between optic lobes were observed in more dorsal layers of the brain. At this level, diffuse ipsilateral projections into the dorsal protocerebrum are also found.

Hornets' MB lobes are clearly different from those described in honeybees and ants (Mobbs, 1982; Mobbs, 1984; Ehmer and Gronenberg 2004; Gronenberg, 2008). In contrast to bees' or ants' MB where the α -lobe extends vertically to the ventral surface of the brain, the *V. velutina* α -lobe points horizontally in a caudal direction and only a fine fiber tract attributed to MB extrinsic neurons (see: Ehmer and Hoy, 2000) extends to the ventral surface (Fig. 3C, E). Moreover, while honeybees' or ants' β -lobes extend horizontally towards the brain midline, the hornet β -lobe is split in two subparts which point dorsally (Fig. 3D, E), in much the same way as previously described in the wasp *Vespula germanica* (Ehmer and Hoy, 2000).

Overall, we did not observe any clear polymorphism in the hornet brain organization except for MB calyces and peduncles which are slightly thinner in males than in females (Fig. 2F, 21.6 % of brain volume in the queen, 23 % in the worker and 15.4 % in the male). The brains of the two female castes are not visually distinguishable.

Antennal lobe organization

Confocal microscopy observations after mass staining of the antennal nerve enabled the segmentation of hornets' antennal lobes into glomerular units ($n = 6$ individuals per caste). We found no difference between female castes in the number of AL glomeruli, with around 269 ± 9 glomeruli in queens (mean \pm SD, $n = 6$) and 264 ± 7 glomeruli in workers ($n = 6$; Mann-Whitney test, $U=10$, non-significant). We observed however a slight sexual dimorphism as the male AL contains 247 ± 6 glomeruli ($n = 6$), i.e. significantly less than in both female castes (Mann-Whitney test, male *vs* queen, $U = 1$, $p < \alpha_{\text{corr}} = 0.025$; male *vs* worker, $U = 1$, $p < \alpha_{\text{corr}} = 0.025$). Based on these 3D-reconstructions, we measured the volumes of glomeruli in the antennal lobes of each caste. Fig. 4A, B, C show individual and average distributions of glomerular volumes in queens, workers and males ($n = 6$ in each group). In all castes, about 80% of glomerular volumes were distributed between 5×10^3 and $100 \times 10^3 \mu\text{m}^3$, most glomeruli displaying a volume around $15 \times 10^3 \mu\text{m}^3$. In workers and queens, the largest glomeruli reached an absolute volume of about $225 \times 10^3 \mu\text{m}^3$, while in males the distribution reached higher values with the largest glomeruli around $1300 \times 10^3 \mu\text{m}^3$. Thus, the three castes seem to share a common pattern of glomerular organization with the exception of a few substantially enlarged glomeruli in males. In order to determine whether these glomeruli are large enough to be termed macroglomeruli, we used a standard quantitative measure that defines outliers with regards to the distribution of glomerular volumes (Fig. 4D). In queens as in workers, the 4 largest glomeruli are located in the most dorsal (2 glomeruli) and in the ventro-lateral regions (2 glomeruli) of the antennal lobe (Fig. 4B, inset). They do not reach the statistical threshold and cannot be considered as macroglomeruli. Similarly sized glomeruli are found at the same positions in males (see black dots Fig. 7). By contrast, the male AL showed several enlarged glomeruli which reached the significance threshold (Fig. 4D and Fig. 5). They were grouped in two clusters: a rostral

cluster contains the largest hornet macroglomerulus (MG1) and two smaller macroglomeruli (MG2, MG3); a ventro-caudal cluster, positioned close to the antennal nerve, contains a group of 4 macroglomeruli. Three of them (MG4, MG5 and MG6) pass the threshold, while the fourth is marginally below the threshold. However, these 4 glomeruli show exactly the same OSN innervation pattern, which is much denser than all the other normal-sized glomeruli in this area. We thus consider this enlarged glomerulus as a possible macroglomerulus, termed MG7. We conclude from these observations that queens and workers have similar antennal lobes without hypertrophied glomeruli, while males possess 7 macroglomeruli distributed in two clusters.

Antennal lobe afferent connection pattern

We next examined the precise projection pattern of OSNs in the antennal lobe of each caste. Because close inspection of projection patterns showed that queen and worker antennal lobes are indiscernible, they are often described together as “female” antennal lobes hereafter. In hornets, the antennal nerve approaches the antennal lobe laterally from the ventral side. As in other Hymenoptera, part of the antennal nerve bypasses the AL and slopes down towards the antennal mechanosensory and motor center (AMMC). OSN axons separate from this main trunk at different depths with various orientations, forming 9 distinct sensory tracts, which we termed T_A to T_I , from the most dorsal to the most ventral (Fig. 6). These tracts give rise to 9 clusters of glomeruli, which display distinctive morphological features. Table 2 gives an overview of glomeruli numbers and volumes for each cluster.

- In the most dorsal part of the AL, 8 glomeruli are innervated by several loose bundle tracts (T_A) which were particularly brightly labeled in most preparations. These glomeruli are identifiable in the three castes by their typical shapes and positional arrangements

(Fig. 6M-O). They are characterized by elongated or bent shapes and receive axon terminals penetrating the entire glomerulus. Their volumes are relatively large, especially for 2 of them that correspond to the largest female glomeruli (black dots in Fig. 7E-F).

- The dorso-caudal region of the antennal lobe harbors a conspicuous cluster of numerous and comparatively smaller glomeruli than in the rest of the AL, rather lightly innervated in their cortex (Fig. 6J-O). This cluster is mostly responsible for the observed variability between sexes and among individuals in the total number of AL glomeruli. Because it was not brightly stained in some preparations, the variability observed in this cluster might be due in part to difficulties for discerning all glomeruli. We counted there 93 ± 7 (mean \pm SD) glomeruli in queens, 89 ± 7 glomeruli in workers and 71 ± 5 glomeruli in males. These glomeruli receive OSN axons from the T_B , which originates from the ventral side and points dorso-medially (Fig. 7E, F).
- The T_C tract runs transversally through the AL, i.e. from the antennal trunk (on the lateral side) towards the dorso-medial side, determining a separation between the T_B cluster and the rest of the AL (Fig. 6G, H, J-L). It sparsely innervates around 15 glomeruli, mostly from their caudal periphery.
- Facing this cluster, the T_D proceeds transversally through the inner dorso-rostral part of the AL and densely innervates about 30 glomeruli in females and 25 glomeruli in males (Fig. 6I-O). We observed there a slight sexual dimorphism, with a thicker tract and relatively larger glomeruli in males, although none of them reached the macroglomerulus volume threshold (Table 2 and Fig. 7E, F).
- More ventrally, we found in both sexes a brightly labeled tract, T_E , which runs in the inner part of the AL, parallel to the T_C . This tract projects medio-dorsally to only 3 glomeruli (Fig. 6E, G-I, and Fig. 7C,D). The deepest T_E glomerulus shows a similar bent

shape as T_A glomeruli and also receives axon terminals in its core region. It is however clearly innervated by the T_E tract.

- The T_F is a thick tract that crosses the AL from the caudo-lateral side to the rostro-medial side and innervates about 20 glomeruli in both males and females (Fig. 6D-F). Despite similar numbers of glomeruli between the sexes, the T_F is much thicker in males. It contains numerous axons that densely project to 3 macroglomeruli termed MG1, MG2 and MG3 above, forming the rostral macroglomerular cluster (Fig. 7C, D).
- Running at the ventral surface of the AL, the T_G separates from the antennal nerve and takes a medio-caudal direction. It innervates around 30 glomeruli mostly from the caudal periphery (Fig. 6A-F). In males, this tract is also thicker than in females and projects into four macroglomeruli close to the antennal nerve (MG4-7), forming the ventro-caudal macroglomerular cluster (Fig. 7A-B).
- The T_H spreads from the antennal nerve to the rostral surface of the AL (Fig. 6A-H). This cluster consists of about 30 relatively large glomeruli and contains among the largest female glomeruli (black dots, Fig. 7A, B).
- Lastly, the T_I extends its axons within about 40 glomeruli from the lateral to the medial side of the AL, forming a cluster sided by T_G and T_H glomeruli (Fig. 6A-C). It innervates glomeruli on the ventral surface and then continues medially towards the dorsal side of the AL (see Fig. 6G-I).

Antennal lobe efferent pathways

Mass staining of the AL with a fluorescent dye revealed that *V. velutina* has a typical hymenopteran olfactory pathway with 5 output PN tracts (Fig. 8A). They seem to correspond to the three multiglomerular (ml-ALT) and two uniglomerular (l- and m-ALT) PN tracts observed in other hymenopteran species (Abel et al., 2001; Kirschner et al., 2006; Zube et al.,

2008). Among the ml-ALT tracts, two leave the AL medially and project transversally to the lateral protocerebrum and the LH. They contribute to a lateral network, and their characteristics are highly similar to the honeybee ml-ACT1 and 2 (Abel et al., 2001; Kirschner et al., 2006). A third ml-ALT tract projects rostrally and bends around the fiber tract extending from the α lobe, sending collaterals towards the peduncle and the lateral network. This tract ramifies in several bundles, ending in the LH and in the caudal protocerebrum. Its trajectory and projections in the protocerebrum are therefore different from those of the honeybee's ml-ACT3 (Kirschner et al., 2006). Next to these ml-ALT PNs, two prominent tracts originate from the dorsal region of the AL and run through the protocerebrum along two widely differing routes, innervating both the LH and the MB calyces. Their itinerary resembles greatly those observed in bees (Abel et al., 2001; Kirschner et al., 2006) and ants (Zube et al., 2008). One median tract (m-ALT) projects rostrally, then follows a medio-lateral route to send first collaterals to both MB calyces and then continues onward to end in the LH. The lateral tract (l-ALT) bends laterally from the exit of the AL, first sends collaterals to the LH and then continues rostrally, eventually forming multiple branches innervating the MBs calyces. We investigated the glomerular connectivity of these tracts in the AL by differentially labeling m-ALT (magenta) and l-ALT (green) PNs ($n = 2$ females, Fig. 8B-H). Like in honeybees and ants, both tracts arborize in different hemilobes of the AL (Fig. 8B) and project to partly segregated areas in the lips (Fig. 8B, C) and the LH (not shown). The l-ALT arborizes in ~ 138 glomeruli in the ventral surface and the rostral region of the AL while the m-ALT arborizes in ~ 127 glomeruli in the dorsal and the caudal regions (Fig. 8D, E). Thus, compared to the honeybee AL, the two hemispheres of the hornet AL seem to be rotated by approximately 45° along the rostro-caudal and medio-lateral axes similarly to what has been observed in the ant *C. floridanus* (Zube et al., 2008). Somata of l-ALT neurons encircle the rostral side of the AL (ISC, Fig. 8D, E, G). By contrast, m-ALT

somata are mainly distributed in two clusters: a dorso-lateral cluster close to the antennal nerve (mSC1, Fig. 8D, E, H) and a rostro-median cluster located next to l-ALT somata (mSC2, Fig. 8D, E, G).

Antennal lobe input-output connectivity

In order to allocate glomerular clusters to either the m- or the l-ALT, we compared OSN and PN stainings of different individuals with the help of the remarkable tract architecture of the hornet AL and of landmark glomeruli (see asterisks and black dots in Fig. 7 and Fig. 8D,E). Table 2 presents the output tract affiliation of the different glomerular clusters. We observed that the T_A cluster is slightly innervated by m-ALT PNs, except for two large landmark glomeruli which were not stained by either of the uniglomerular tracts. Dorso-caudal clusters, T_B and T_C , clearly belong to the m-subsystem whereas ventro-rostral clusters T_D , T_F , T_H and T_I clearly belong to the l-subsystem. The T_E cluster is innervated by m-ALT PNs except for one glomerulus that receives processes from both m- and l-ALT neurons. Glomeruli of the T_G are divided in 2 groups: about 24 glomeruli belong to the m-subsystem and 9 belong to the l-subsystem.

Common features of the hymenopteran antennal lobe

When studying the input-output connectivity of the hornet antennal lobe, we noticed conspicuous similarities with the antennal lobes of two well-described hymenopteran species, the honeybee *Apis mellifera* (Apidae) and the carpenter ants *Camponotus* sp. (Formicidae). Several glomerular clusters presented strikingly similar features in the different species, which led us to propose a common framework for describing these antennal lobes. Table 3 presents the putative homologies between the antennal lobes of the three model species, while

Table 4 lists the typical features defining each cluster type. The most striking observation is that all glomerular clusters found in honeybees and in ants have an equivalent cluster in hornets, while some clusters found in ants are not found in bees and vice versa. For observing these homologies in the best conditions, the ALs should be oriented similarly in the three species, with the antennal nerve entrance on the same axis, and the separation plane between l-ALT and m-ALT hemilobes in the same orientation across species. We detail below the clues supporting the proposed homologies:

Glomerular cluster T_A is the most dorsal in hornets and presents very distinctive features, found in all three species. It contains a few large glomeruli with peculiar shapes and positional arrangements. It mostly belongs to the m-ALT subsystem but, remarkably, two glomeruli are neither innervated by m-ALT nor by l-ALT PNs. In honey bees and carpenter ants the most dorsal cluster (T_4 in *Apis mellifera*, T_7 in *Camponotus*) shows the same features, which led previous studies to already suggest their homology (Zube et al., 2008; Nakanishi et al., 2010). The “necklace” organization of glomeruli T_A -01, 03, 05, 06 08 in hornets greatly resembles that of glomeruli D01, D03, D05, D06, D08 in honeybees (Fig. 9A; compare to Fig. 5B in Kirschner et al., 2006). The homology is even more remarkable between hornet’s T_A -02 glomerulus (Fig. 9A) and honeybees’ D02 glomerulus (see Fig. 3H-I in Kirschner et al., 2006) as both are egg-shaped, positioned close to the antennal nerve, and lack any uniglomerular PN arborization.

The T_B is a dorso-medial cluster, partly segregated from the main part of the AL, which flanks the antennal nerve and generally contains smaller glomeruli than the main AL, innervated by m-ALT PNs (Fig. 9A). These features clearly correspond to those of the T_6 cluster of *Camponotus* workers (compare to Fig. 2C in Zube et al., 2008) and are also found in the T_{3b} of *Apis mellifera*, although it contains much fewer glomeruli than in the other species (see Fig. 4A-C in Kirschner et al., 2006).

Glomeruli belonging to the T_C also belong to the m-ALT subsystem. They occupy a caudo-medial position within the antennal lobe of hornets and mostly receive sensory innervations from the caudal periphery of the AL. These features fit with those of the honeybee $T3c$ and the ant $T5$ clusters which have similar PNs arborization, locations and afferent innervations (Fig. 9B; compare to Fig. 3G in Kirschner et al., 2006; see also contralateral view in Fig. 2J-O in Nakanishi et al., 2010).

The T_D glomeruli belong to the l-ALT subsystem and receive axon terminals from a highly characteristic thick tract which proceeds along the inner lateral part of the AL (Fig. 9B). Similar features were observed in *Camponotus* ants with the $T4$ tract (compare to Fig. 1C in Zube et al., 2008) but we did not find any clear correspondence in *Apis mellifera*.

Conversely, two other clusters, T_E and T_F , had clear correspondences in *Apis mellifera* (respectively with $T2$ and $T1$) but not in carpenter ants. The honeybee $T2$ was considered as homologous to the hornet T_E because in both species this sensory tract runs through the inner medial part of the AL and project to very few glomeruli with singular shapes (Fig. 9C; compare to Fig. 3E in Kirschner et al., 2006). This homology is strongly supported by the features of a landmark glomerulus. The *Apis mellifera* B02 glomerulus is innervated by both l- and m-ALT PNs and receives sensory axon terminals in both its cortex and its core (see Fig. 4F,H in Nishino et al., 2009). The hornet T_E -01 glomerulus shows exactly the same features (Fig. 9C).

On the other hand, the putative homology between the hornet T_F and the *Apis mellifera* $T1$ is based on their similar affiliation to the l-ALT subsystem and to the conspicuous sensory tract which projects through the midline of the AL (Fig. 9C; compare to Fig. 3E in Kirschner et al., 2006). In both species, it exhibits a clear sex dimorphism, being much thicker in males than in females and containing several macroglomeruli (Fig. 5B; see Fig. 5D-F in Nishino et al., 2009).

In *V. velutina* as well as in *Apis mellifera* and carpenter ants, only one glomerular cluster is shared between the l- and the m-ALT subsystems, some of its glomeruli containing only l-ALT processes, others only m-ALT processes (they are termed T_G, T3a and T3 respectively in the three species). This cluster is located in the medio-caudal part of the AL in all species and contains glomeruli that are mostly innervated from their medial periphery (Fig. 9D; compare to Fig. 1A in Zube et al., 2008; see also Fig. 3C-F in Kirschner et al., 2006).

Visually, the ventral surface of the hornet AL bears a strong resemblance with that of the carpenter ant, exhibiting similar clusters (Fig. 9D; compare to Fig. 1A and 2B in Zube and Rössler, 2008). Glomeruli of the lateral surface receive sensory afferences from the T_H in *V. velutina* or the T2 in *Camponotus sp.* and belong to the l-ALT. Glomeruli from the hornet T_I or T1 cluster in ants also belong to the l-ALT and are innervated by a sensory tract which first projects to the rostral part of the AL before sloping down dorsally (Fig. 9D; compare to contralateral view Fig. 2A-F in Nakanishi et al., 2010). No equivalent of these clusters is however present in honeybees.

All in all, these observations suggest that the hornet antennal lobe presents both honeybee and ant features.

Discussion

We studied the neuronal olfactory pathway of the hornet brain and its sex and caste-specific adaptations. Whole brain staining revealed that the overall organization of the *Vespa velutina* brain is highly similar in the two sexes and between female castes. Whereas the morphology of the hornet MBs appears distinct from that of other Hymenoptera, we found homologous structures and the same subdivision of olfactory and visual inputs (lips and collars) in the MB calyces. Our data also show that the antennal lobe of *V. velutina* consists of ~265 glomeruli

distributed in 9 clusters innervated by distinct antennal sensory tracts. The number of glomeruli and their volume distribution are similar between the female castes. The antennal lobe of males contains fewer glomeruli but harbors 7 macroglomeruli organized in 2 clusters. We observed 5 output (PN) tracts that arborize in the AL and project to higher order centers: two prominent tracts arborize in distinct antennal lobe hemilobes and project towards partly segregated areas of MB calyces and LH, in a reverse order. Three relatively smaller output tracts project through the protocerebrum towards the LH. Lastly, the input-output relationships of hornets' ALs display striking similarities with those of honey bees and ants, allowing a common framework for describing the olfactory pathway in these species.

Low dimorphism in the hornet brain

Several observations we made in hornets differ substantially from what is known in the other described Hymenoptera. Firstly, a marked sex dimorphism within the central nervous system has been reported in many hymenopteran species and was assumed to be impelled by sexual selection (Ehmer and Gronenberg, 2004; Nishikawa 2008; Streinzer et al., 2013; Roselino et al., 2015). The competition between males could act as a selective pressure on the sensory system for improving the localization of fertile females (Anderson and Iwasa, 1996). To assess a potential differential investment of the different sexes in particular sensory systems, the relative size of brain neuropils has been compared between males and females in several eusocial species. In these species, like in *Apis mellifera* (honey bee), *Camponotus japonicus* (carpenter ant), *Atta vollenweideri* (leaf-cutting ant) or *Melipona scutellaris* (stingless bee), males present larger optic lobes (medulla and/or lobula) than females, suggesting sex differences in visual processing (Gronenberg and Hölldobler, 1999; Ehmer and Gronenberg, 2004; Nishikawa et al., 2008; Kuebler et al., 2010; Streinzer et al., 2013; Roselino et al., 2015). It was suggested that this sex-specific sensory adaptation is related to

the importance of vision to detect and pursue fast movements of fertile females during mating flights (Ehmer and Gronenberg, 2004). Our data on the hornet *V. velutina* show that enlarged optic lobes in males are not a general feature of social Hymenoptera, as we did not find conspicuous size differences between males and females. In fact, behavioral observations in hornets in general, and *V. velutina* in particular, indicate that mating occurs on the nests or other solid substrate but not in flight (Matsuura and Yamane, 1990; Monceau et al., 2014). These observations are in accordance with a less crucial role of vision in hornet males for finding their sexual partners than in other Hymenoptera. Alternatively, the hornet brain could be generally preadapted for highly-demanding visual tasks (like catching preys on the fly), so that the system is already sufficient for processing all the information relevant to mating.

Secondly, fewer antennal lobe glomeruli and smaller MBs in males are ubiquitous features in social Hymenoptera and were assumed to be linked to a smaller behavioral repertoire in males (Arnold et al., 1985; Ehmer and Gronenberg, 2004; Kuebler et al., 2010; Smith et al., 2010; Streinzer et al., 2013). Typically, a lower number of glomeruli suggests a lower number of expressed olfactory receptors and can accordingly be linked to reduced olfactory discrimination abilities compared to females. In addition, smaller MBs, brain centers crucial for multimodal sensory integration, memory, and complex learning (Heisenberg, 1998; Farris, 2005; Strausfeld et al., 2009; Devaud et al., 2015), suggest lower cognitive capabilities in males. A recent comparative study underlined a less pronounced sexual dimorphism in number of glomeruli and MB size in solitary than in social bees (Streinzer et al., 2013). In contrast with males of eusocial species which benefit from colonial altruism and only leave the colony for mating flights, males of solitary species require a higher behavioral plasticity, which might be responsible for such lower sex dimorphism (Stubblefield and Seger, 1994). Contrary to this general rule, we observed only ~20 (7%) less glomeruli in *V. velutina* males compared to females, which is clearly low compared to the approximately ~30-40% reduction

found in honey bees and carpenter ants (Arnold et al., 1985; Zube and Rössler, 2008; Nishino et al., 2009; Nakanishi et al., 2010). In the same way, the calyces and peduncle of hornet male MBs were only slightly thinner than those of females (see also Molina and O'Donnell, 2008). In hornets, males were observed to be rejected from their colony and to then perform foraging by their own means (Monceau et al., 2013, 2014). Following these observations, a less pronounced sex dimorphism in the hornet brain could be attributed to a more elaborate male behavioral repertoire than in other species.

Hornet macroglomeruli

To estimate the presence of enlarged glomeruli in the antennal lobe of *V. velutina*, we measured glomerular volumes using confocal microscopy and 3D reconstruction. We did not find any macroglomerulus in hornet females but the male AL presented 2 clusters with 7 strongly enlarged glomeruli. These glomerular clusters were densely innervated by OSNs, resulting in thicker T_F and T_G tracts in males than in females. While female macroglomeruli are adaptations related to the colony lifestyle of eusocial insects, male macroglomeruli are found throughout insects because they are involved in mating (Arnold et al., 1985; Hanson et al., 1992; Nishikawa et al., 2008; Nishino et al., 2012). In many species, like in moths or cockroaches, male-specific macroglomeruli are located in the caudal region of the antennal lobe, close to the entrance of the antennal nerve (Rospars and Chambille, 1986; Skiri et al., 2005; Nishino et al., 2012; Das and Faddamiro, 2013). In the ant *Camponotus japonicus*, two macroglomeruli at similar locations were attributed to the T3 tract and were assumed to have a sex pheromone-receptive function (Nakanishi et al., 2010). By contrast, in honey bee drones, 3 macroglomeruli attributed to the T1 tract are located rostrally, one of which specifically responds to the sex pheromone compound 9-ODA (Arnold et al., 1985; Sandoz, 2006; Nishino et al., 2009). Compared to other species, hornet males present numerous

macroglomeruli of both types: an ant-like cluster of 4 ventro-caudal macroglomeruli (T_G), located close to the entrance of the antennal nerve and a honey bee-like cluster of 3 rostral macroglomeruli (T_F). Such sex-specific investment in several hypertrophied glomerular structures should be connected to a crucial role played by several odorants in the mating behavior of *V. velutina* males. Observation of the mating behavior of a related species, *Vespa crabro*, highlighted the existence of at least two different pheromones (Ayasse et al., 2001). Hornet females produce a long range pheromone that attracts males from long distances (Ono and Sasaki, 1987; Spiewok et al., 2006). In addition, a contact pheromone on the queen's thorax elicits copulatory behavior in males (Batra, 1980). One possibility is that one of the macroglomerulus clusters of the male hornet AL would be involved in long-range detection of the sex attractant pheromone while the second would process contact recognition cues such as fertility signals. More extensive data on the mating behavior of *V. velutina* and on the implicated chemical signals are needed for substantiating these hypotheses.

A common reference for the hymenopteran antennal lobe

Despite the considerable variations observed in the number of glomeruli across hymenopteran species, previous studies already pointed out striking similarities, as well as important differences, in the organization of ants' and honey bees' ALs. The most remarkable similarity between these species resides in the subdivision of the AL in two hemilobes of almost equal size, separately innervated by two prominent output tracts (m- and l-ALT) (Abel et al., 2001; Galizia and Rössler, 2010; Rössler and Zube, 2011). Such a dual olfactory pathway has been found in diverse taxa among Hymenoptera, except in some sawflies, suggesting its initial appearance in basal Hymenoptera (Dacks and Nighorn, 2011; Rössler and Zube 2011). In accordance with these observations, we show that Vespidae also possess such a dual pathway, which appears, like in the ant *Camponotus floridanus*, rotated by 45° on the rostro-caudal and

medio-lateral axis compared to that of the honey bee *Apis mellifera*. We found however other significant similarities between the antennal lobes of these three species, which we attempted to integrate within a common framework (Table 3). Generally, the homologies we propose fit with and expand those proposed in an earlier work comparing bees and carpenter ants (Zube et al., 2008). Based on OSN projection patterns, we observed that the hornet antennal lobe contains 9 clusters, each receiving differentially-oriented branches of the antennal nerve. Using similar classification rules, the antennal lobe of honey bees has been subdivided in 6 glomerular clusters (T1-T4, taking into account the T3a-c subdivision; Galizia et al., 1999; Kirschner et al., 2006; Nishino et al., 2009) while 7 clusters have been identified in carpenter ants (Zube et al., 2008; Nakanishi et al., 2010). The possible homologies we described are mostly based on neuroanatomical features related to glomerular output connectivity, OSN tract innervation patterns, cluster localizations and average glomerular size. These features, alone, may not be sufficient to unambiguously demonstrate these homologies, and further comparative studies including functional data from these clusters would certainly be helpful for proving their validity. However, for some of them, available functional and neuroanatomical data already strongly support homologies across species. For instance, the T_A cluster contains a few (6-10) large glomeruli located on the most dorsal region of the AL, and harbor typical whole-glomerulus OSN projections, features which fit perfectly with those of the honey bee T4 cluster (7 glomeruli, Kirschner et al., 2006; Nishino et al., 2009) and of the ant T7 cluster (6 to 10 glomeruli, Zube et al., 2008; Nakanishi et al., 2010). These glomeruli are often described as homologous to the T10 cluster of the cockroach, containing hygro/thermo sensitive neurons (Nishino et al., 2009; Watanabe et al., 2010), so that homologies for this cluster may reach beyond Hymenoptera. Another strongly-supported homology concerns the T_B cluster. It is characterized in hornets by many small glomeruli forming a tight group slightly segregated from the main AL. This cluster was already

observed in the wasp *Polistes gallicus*, in the form of a glomerular compartment with distinct neuropeptide activity compared to the main AL (Masson and Strambi, 1977). This compartment corresponds to the T6 cluster of carpenter ants (Zube et al., 2008; Nakanishi et al., 2010). This cluster is female-specific in ants and bees and noticeably receives olfactory neurons housed in basiconic sensilla (Zube and Rössler, 2008; Kelber et al., 2010; Nakanishi et al., 2010; Nishikawa et al., 2012; Kropf et al., 2014). It is currently thought that these glomeruli may be involved in the processing of cuticular hydrocarbons, which are crucial for nestmate recognition in social insect colonies (Ozaki et al., 2005; Sharma et al., 2015). We recently obtained neuroanatomical and functional data suggesting a similar role in hornets, which supports the T_B homology (Couto et al., in prep).

For other clusters with less conspicuous features, homologies could be more difficult to discern and demonstrate. The present data in hornets allows however resolving some previous uncertainties in the comparison between honey bees and ants. Thus, the *Camponotus floridanus* T1, T2 and T4 clusters were all suggested as possible homologous clusters to the honey bee T1 cluster (Zube et al., 2008). The honey bee T1 projects rostrally, through the middle of the AL, and in males, contains 3 macroglomeruli. These features are strikingly similar to those of the hornet T_F (Kirschner et al., 2006; Nishino et al., 2009). In addition, we found other, more similar clusters to the ants' T1, T2 and T4 tracts in the hornet AL (T_I, T_H and T_D, respectively). Our current view is thus that none of the carpenter ant clusters is homologous to the T1 cluster of honey bees. Future work should strive to provide additional data allowing to corroborate the putative homologies we proposed. In this prospect, a systematic investigation of sensillar equipment (morphological types of olfactory sensilla) on the antenna, and their antennal lobe afferences in the different species (see Kropf et al., 2014 and Kelber et al., 2006), along with systematic immunohistochemistry for the main

neurotransmitters and neuropeptides (Masson and Strambi, 1977; Zube and Rössler, 2008; Dacks et al., 2010; Siju et al., 2014), could provide pivotal clues for testing our model.

New insights into the evolution of the hymenopteran antennal lobe

Because the olfactory system is at the interface between the animal and its environment, it receives strong selection pressures, which induce the gain or loss of subcircuits depending on changes in the relative importance of particular chemical stimuli in the biology of the species (Ramdya and Benton, 2010). Glomerular clusters are conspicuous entities in the hymenopteran antennal lobe but it is still unclear whether or not different clusters are systematically involved in the detection of different odorant classes. As detailed above, for some remarkable clusters like the T_A or T_B , current data points in this direction. For most other clusters, however, it may not be so clear cut, as even different AL hemilobes show strongly overlapping odor response spectra (Carcaud et al., 2012; Brill et al., 2013, but see Carcaud et al., 2015). It is nevertheless possible that within each cluster, OSNs express groups of closely-related olfactory receptor (OR) genes, as suggested by data in fruit flies. In this insect, ORs genes with highest sequence similarity tend to be expressed in OSNs targeting neighbor glomeruli, suggesting such lineage constraints on OSN projection patterns (Couto et al., 2005; Vosshall et al., 2005). This may appear through the action of specific transcription factor genes controlling OSN axon targeting (Komiyama et al., 2004; Tichy et al., 2008). Thus, the antennal sensory tract ramifications observed in Hymenoptera might be the result of genetically encoded axonal-guidance factors, which could participate in a coarse odotopic representation of odors in the antennal lobe.

The evolution of the antennal lobe is thought to entail a continuous ‘birth-and-death’ process of ORs, inducing the budding/pruning of glomeruli within each cluster, and, eventually, of whole clusters (Ramdya and Benton, 2010). The comparative analysis of AL

neuroanatomy, and the homologies we observed, could help retracing the evolution of the AL in Hymenoptera. At this stage, the phylogeny of Hymenoptera is not totally resolved and remains controversial (Brothers, 1999; Pilgrim et al., 2008; Heraty et al., 2011; Sharkey et al., 2012). However, according to a recent phylogeny of stinging Hymenoptera, supported by extensive genomic and transcriptomic data sets (Johnson et al., 2013), Vespidae would be more basal among aculeates than Formicidae and Apoidea which would be sister groups. If this phylogeny is confirmed, then one could speculate that the common ancestor of Vespidae, Formicidae and Apoidea harbored a relatively complex AL with many sensory tract subdivisions, and that different secondary losses took place in Formicidae (T_E and T_F) and Apoidea (T_D , T_H and T_I). Clearly, these stimulating hypotheses can only be substantiated through the long-term study of AL neuroanatomical features and input-output relationships in a wider range of hymenopteran taxa. Interestingly, we note that the most strongly conserved clusters (T_A , T_B and T_C) are related to the m-ALT PN tract, while the clusters that are related to the l-ALT output tract strongly vary among species (see Table 3). It seems remarkable that this output tract is the one that diverged more recently, probably in some basal Hymenoptera, while the m-ALT is the ancestral tract (Rössler and Galizia, 2010). If confirmed in other hymenopteran taxa, this could indicate that the invention of the l-ALT tract has provided Hymenoptera with a highly adaptable and plastic olfactory subsystem, potentially instrumental for their adaptation to a wide range of ecological niches and their ecological success, while basic biological functions would be secured by the other, ancestral tract.

Acknowledgements

We thank O. Bonnard for hornet collection and K. Monceau for helpful discussion on the biology of hornets. We are indebted to J. Rybak and C. Kelber for helpful technical advice and to A.C. Roselino and F. Bastin for insightful discussion.

Literature Cited

- Abel R, Rybak J, Menzel R. 2001. Structure and response patterns of olfactory interneurons in the honeybee, *Apis mellifera*. *The J Comp Neur* 437:363-383.
- Ai H, Kanzaki R. 2004. Modular organization of the silkworm antennal lobe macroglomerular complex revealed by voltage-sensitive dye imaging. *J Exp Biol* 207:633-644.
- Andersson M, Iwasa Y. 1996. Sexual selection. *Trends Ecol Evol* 11:53-58.
- Anton S, Homberg U. 1999. Antennal lobe structure. In: Hansson BS, editor. *Insect Olfaction*: Springer Heidelberg. p 97-124.
- Anton S, Ignell R, Hansson BS. 2002. Developmental changes in the structure and function of the central olfactory system in gregarious and solitary desert locusts. *Microsc Res Tech* 56:281-291.
- Arca M, Mougél F, Guillemaud T, Dupas S, Rome Q, Perrard A, Muller F, Fossoud A, Capdevielle-Dulac C, Torres-Leguizamon M. 2015. Reconstructing the invasion and the demographic history of the yellow-legged hornet, *Vespa velutina*, in Europe. *Biological Invasions* 17:1-15.
- Arnold G, Budharugsa S, Masson C. 1988. Organization of the antennal lobe in the queen honey bee, *Apis mellifera* L. (Hymenoptera : Apidae). *Int J Insect Morphol Embryol* 17:185-195.
- Arnold G, Masson C, Budharugsa S. 1985. Comparative study of the antennal lobes and their afferent pathway in the worker bee and the drone (*Apis mellifera*). *Cell Tissue Res* 242:593-605.
- Ayasse M, Paxton RJ, Tengö J. 2001. Mating behavior and chemical communication in the order hymenoptera. *Annu Rev Entomol* 46:1:31-78.
- Batra SWT. 1980. Sexual behavior and pheromones of the European hornet, *Vespa crabro germana* (Hymenoptera: Vespidae). *J Kans Entomol Soc* 53:461-469.
- Brill MF, Rosenbaum T, Reus I, Kleineidam CJ, Nawrot MP, Rössler W. 2013. Parallel processing via a dual olfactory pathway in the honeybee. *J Neurosci* 33:2443-2456.
- Brodmann J, Twele R, Francke W, Yi-bo L, Xi-qiang S, Ayasse M. 2009. Orchid mimics honey bee alarm pheromone in order to attract hornets for pollination. *Curr Biol* 19:1368-1372.
- Brothers DJ. 1999. Phylogeny and evolution of wasps, ants and bees (Hymenoptera, Chrysidoidea, Vespoidea and Apoidea). *Zool Scr* 28:233-250.
- Bruschini C, Cervo R, Turillazzi S. 2010. Chapter nineteen - Pheromones in social wasps. In: Gerald L, editor. *Vitam Horm: Academic Press*. p 447-492.
- Burrows M, Boeckh J, Esslen J. 1982. Physiological and morphological properties of interneurons in the deutocerebrum of male cockroaches which respond to female pheromone. *J Comp Physiol A* 145:447-457.
- Carcaud J, Hill T, Giurfa M, Sandoz JC. 2012. Differential coding by two olfactory subsystems in the honeybee brain. *J neurophysiol* 108:1106-1121.
- Carcaud J, Giurfa M, Sandoz JC. 2015. Differential combinatorial coding of pheromones in two olfactory subsystems of the honey bee brain. *J Neurosci* 35(10): 4157-4167.
- Cardinal S, Danforth BN. 2011. The Antiquity and Evolutionary History of Social Behavior in Bees. *PLoS ONE* 6:e21086.
- Clifford M, Riffell J. 2013. Mixture and odorant processing in the olfactory systems of insects: a comparative perspective. *J Comp Physiol A* 199:911-928.
- Couto A, Alenius M, Dickson BJ. 2005. Molecular, anatomical, and functional organization of the *Drosophila* olfactory system. *Curr Biol* 15:1535-1547.

- Couto A, Monceau K, Bonnard O, Thiéry D, Sandoz JC. 2014. Olfactory attraction of the hornet *Vespa velutina* to honeybee colony odors and pheromones. PLoS ONE 9:e115943.
- Dacks AM, Nighorn AJ. 2011. The organization of the antennal lobe correlates not only with phylogenetic relationship, but also life history: a basal hymenopteran as exemplar. Chem Senses 36:209-220.
- Dacks AM, Reisenman CE, Paulk AC, Nighorn AJ. 2010. Histamine-immunoreactive local neurons in the antennal lobes of the hymenoptera. J Comp Neurol 518(15): 2917-2933.
- Das P, Fadamiro H. 2013. Species and sexual differences in antennal lobe architecture and glomerular organization in two parasitoids with different degree of host specificity, *Microplitis croceipes* and *Cotesia marginiventris*. Cell Tissue Res 352:227-235.
- Devaud J-M, Papouin T, Carcaud J, Sandoz J-C, Grünewald B, Giurfa M. 2015. Neural substrate for higher-order learning in an insect: Mushroom bodies are necessary for configural discriminations. Proc Natl Acad Sci USA 112:5854-5862.
- Edwards R. 1980. Social wasps. Their biology and control: Rentokil Ltd.
- Ehmer B, Gronenberg W. 2004. Mushroom body volumes and visual interneurons in ants: comparison between sexes and castes. J Comp Neurol 469:198-213.
- Ehmer B, Hoy R. 2000. Mushroom bodies of vespids wasps. J Comp Neurol 416:93-100.
- Farris SM. 2005. Evolution of insect mushroom bodies: old clues, new insights. Arth Struct Dev 34:211-234.
- Flanagan D, Mercer AR. 1989. An atlas and 3-D reconstruction of the antennal lobes in the worker honey bee, *Apis mellifera* L. (Hymenoptera : Apidae). Int J Insect Morphol Embryol 18:145-159.
- Flögel JHL. 1878. Über den einheitlichen Bau des Gehirns in den verschiedenen Insecten-Ordnungen. Z Wiss Zool Suppl 30:556-592.
- Galizia CG, McIlwraith SL, Menzel R. 1999. A digital three-dimensional atlas of the honeybee antennal lobe based on optical sections acquired by confocal microscopy. Cell Tissue Res 295:383-394.
- Galizia CG, Rössler W. 2010. Parallel olfactory systems in insects: anatomy and function. Annu Rev Entomol 55:399-420.
- Groh C, Rössler W. 2008. Caste-specific postembryonic development of primary and secondary olfactory centers in the female honeybee brain. Arth Struct Dev 37:459-468.
- Gronenberg W. 2008. Structure and function of ant (Hymenoptera: Formicidae) brains: Strength in numbers. Myrmecological News 11:25-36.
- Gronenberg W, Hölldobler B. 1999. Morphologic representation of visual and antennal information in the ant brain. J Comp Neurol 412:229-240.
- Guidobaldi F, May-Concha IJ, Guerenstein PG. 2014. Morphology and physiology of the olfactory system of blood-feeding insects. J Physiology-Paris 108:96-111.
- Hansson B, Ljungberg H, Hallberg E, Lofstedt C. 1992. Functional specialization of olfactory glomeruli in a moth. Science 256:1313-1315.
- Hansson BS, Anton S. 2000. Function and morphology of the antennal lobe: new developments. Annu Rev Entomol 45:203-231.
- Hansson Bill S, Stensmyr Marcus C. 2011. Evolution of insect olfaction. Neuron 72:698-711.
- Hanström B. 1928. In Vergleichende Anatomie des Nervensystems der wirbellosen Tiere: Springer-Verlag.
- Heisenberg M. 1998. What Do the Mushroom Bodies Do for the Insect Brain? An Introduction. Learn Memory 5:1-10.

- Heraty J, Ronquist F, Carpenter JM, Hawks D, Schulmeister S, Dowling AP, Murray D, Munro J, Wheeler WC, Schiff N, Sharkey M. 2011. Evolution of the hymenopteran megaradiation. *Mol Phylogenet Evol* 60:73-88.
- Hildebrand JG, Shepherd GM. 1997. Mechanisms of olfactory discrimination: Converging evidence for common principles across phyla. *Annu Rev Neurosci* 20:595-631.
- Hines HM, Hunt JH, O'Connor TK, Gillespie JJ, Cameron SA. 2007. Multigene phylogeny reveals eusociality evolved twice in vespid wasps. *Proc Natl Acad Sci U S A* 104:3295-3299.
- Hughes WOH, Oldroyd BP, Beekman M, Ratnieks FLW. 2008. Ancestral monogamy shows kin selection is key to the evolution of eusociality. *Science* 320:1213-1216.
- Hunt JH. 2007. *The evolution of social wasps*: Oxford University Press.
- Ibba I, Angioy A, Hansson B, Dekker T. 2010. Macrogglomeruli for fruit odors change blend preference in *Drosophila*. *Naturwissenschaften* 97:1059-1066.
- Ignell R. 2001. Monoamines and neuropeptides in antennal lobe interneurons of the desert locust, *Schistocerca gregaria*: an immunocytochemical study. *Cell Tissue Res* 306:143-156.
- Ignell R, Anton S, Hansson BS. 2001. The antennal lobe of orthoptera – anatomy and evolution. *Brain Behav Evol* 57:1-17.
- Ikan R, Gottlieb R, Bergmann ED, Ishay J. 1969. The pheromone of the queen of the Oriental hornet, *Vespa orientalis*. *J Insect Physiol* 15:1709-1712.
- Ishay J. 1973. Thermoregulation by social wasps: behavior and pheromones. *Trans N Y Acad Sci* 35:447-462.
- Johnson Brian R, Borowiec Marek L, Chiu Joanna C, Lee Ernest K, Atallah J, Ward Philip S. 2013. Phylogenomics Resolves Evolutionary Relationships among Ants, Bees, and Wasps. *Curr Biol* 23:2058-2062.
- Kelber C, Rössler W, Kleineidam CJ. 2006. Multiple olfactory receptor neurons and their axonal projections in the antennal lobe of the honeybee *Apis mellifera*. *J Comp Neurol* 496:395-405.
- Kelber C, Rössler W, Kleineidam CJ. 2010. Phenotypic plasticity in number of glomeruli and sensory innervation of the antennal lobe in leaf-cutting ant workers (*A. vollenweideri*). *Dev Neurobiol* 70:222-234.
- Kelber C, Rössler W, Roces F, Kleineidam CJ. 2009. The antennal lobes of fungus-growing ants (Attini): neuroanatomical traits and evolutionary trends. *Brain Behav Evol* 73:273-284.
- Kirschner S, Kleineidam CJ, Zube C, Rybak J, Grünewald B, Rössler W. 2006. Dual olfactory pathway in the honeybee, *Apis mellifera*. *J Comp Neurol* 499:933-952.
- Kleineidam C, Rössler W. 2009. Adaptations in the olfactory system of social Hymenoptera. In: Gadau J, Fewell J, Wilson E, editors. *Organization of insect societies: from genome to sociocomplexity*: Harvard University Press: 195-219.
- Kleineidam CJ, Obermayer M, Halbich W, Rössler W. 2005. A Macrogglomerulus in the antennal lobe of leaf-cutting ant workers and its possible functional significance. *Chem Senses* 30:383-392.
- Komiyama T, Carlson JR, Luo L. 2004. Olfactory receptor neuron axon targeting: intrinsic transcriptional control and hierarchical interactions. *Nat Neurosci* 7:819-825.
- Kropf J, Kelber C, Bieringer K, Rössler W. 2014. Olfactory subsystems in the honeybee: sensory supply and sex specificity. *Cell Tissue Res* 357:583-595.
- Kuebler LS, Kelber C, Kleineidam CJ. 2010. Distinct antennal lobe phenotypes in the leaf-cutting ant (*Atta vollenweideri*). *J Comp Neurol* 518:352-365.

- Martin JP, Beyerlein A, Dacks AM, Reisenman CE, Riffell JA, Lei H, Hildebrand JG. 2011. The neurobiology of insect olfaction: Sensory processing in a comparative context. *Prog Neurobiol* 95:427-447.
- Masson C, Strambi C. 1977. Sensory antennal organization in an ant and a wasp. *Journal Neurobiol* 8:537-548.
- Matsuura M, Yamane S. 1990. *Biology of the vespine wasps*: Springer Verlag.
- Mobbs PG. 1982. The Brain of the Honeybee *Apis Mellifera*. I. The Connections and Spatial Organization of the Mushroom Bodies. *Phil Trans R Soc Lond B* 298:309-354.
- Mobbs PG. 1984. Neural networks in the mushroom bodies of the honeybee. *J Insect Physiol* 30:43-58.
- Molina Y, O'Donnell S. 2008. Age, sex, and dominance-related mushroom body plasticity in the paperwasp *Mischocyttarus mastigophorus*. *Dev Neurobiol* 68:950-959.
- Monceau K, Bonnard O, Thiéry D. 2013. Relationship between the age of *Vespa velutina* workers and their defensive behaviour established from colonies maintained in the laboratory. *Insect Soc* 60:437-444.
- Monceau K, Bonnard O, Thiéry D. 2014. *Vespa velutina*: a new invasive predator of honeybees in Europe. *J Pest Sci* 87:1-16.
- Mysore K, Subramanian KA, Sarasij RC, Suresh A, Shyamala BV, VijayRaghavan K, Rodrigues V. 2009. Caste and sex specific olfactory glomerular organization and brain architecture in two sympatric ant species *Camponotus sericeus* and *Camponotus compressus* (Fabricius, 1798). *Arth Struct Dev* 38:485-497.
- Nakanishi A, Nishino H, Watanabe H, Yokohari F, Nishikawa M. 2010. Sex-specific antennal sensory system in the ant *Camponotus japonicus*: glomerular organizations of antennal lobes. *J Comp Neurol* 518:2186-2201.
- Nishikawa M, Nishino H, Misaka Y, Kubota M, Tsuji E, Satoji Y, Ozaki M, Yokohari F. 2008. Sexual dimorphism in the antennal lobe of the ant *Camponotus japonicus*. *Zoolog Sci* 25:195-204.
- Nishikawa M, Watanabe H, Yokohari F. 2012. Higher brain centers for social tasks in worker ants, *Camponotus japonicus*. *J Comp Neurol* 520:1584-1598.
- Nishino H, Iwasaki M, Kamimura I, Mizunami M. 2012. Divergent and convergent projections to the two parallel olfactory centers from two neighboring, pheromone-receptive glomeruli in the male American cockroach. *J Comp Neurol* 520:3428-3445.
- Nishino H, Nishikawa M, Mizunami M, Yokohari F. 2009. Functional and topographic segregation of glomeruli revealed by local staining of antennal sensory neurons in the honeybee *Apis mellifera*. *J Comp Neurol* 515:161-180.
- O'Donnell S, Donlan NA, Jones TA. 2004. Mushroom body structural change is associated with division of labor in eusocial wasp workers (*Polybia aequatorialis*, Hymenoptera: Vespidae). *Neurosci Lett* 356:159-162.
- O'Donnell S, Clifford M, Molina Y. 2011. Comparative analysis of constraints and caste differences in brain investment among social paper wasps. *Proc Natl Acad Sci USA* 108:7107-7112.
- O'Donnell S, Bulova SJ, DeLeon S, Khodak P, Miller S, Sulger E. 2015. Distributed cognition and social brains: reductions in mushroom body investment accompanied the origins of sociality in wasps (Hymenoptera: Vespidae). *Proc R Soc Lond B Biol Sci : Biological Sciences* 282: 20150791.
- Oi Cintia A, Van Oystaeyen A, Caliar Oliveira R, Millar Jocelyn G, Verstrepen Kevin J, van Zweden Jelle S, Wenseleers T. 2015. Dual Effect of Wasp Queen Pheromone in Regulating Insect Sociality. *Curr Biol* 25:1638-1640.
- Ono M, Igarashi T, Ohno E, Sasaki M. 1995. Unusual thermal defence by a honeybee against mass attack by hornets. *Nature* 377:334-336.

- Ono M, Sasaki M. 1987. Sex pheromones and their cross-activities in six Japanese sympatric species of the genus *Vespa*. *Insect Soc* 34:252-260.
- Ono M, Terabe H, Hori H, Sasaki M. 2003. Insect signalling: components of giant hornet alarm pheromone. *Nature* 424:637-638.
- Ozaki M, Wada-Katsumata A, Fujikawa K, Iwasaki M, Yokohari F, Satoji Y, Nisimura T, Yamaoka R. 2005. Ant Nestmate and Non-Nestmate Discrimination by a Chemosensory Sensillum. *Science* 309:311-314.
- Perrard A, Villemant C, Carpenter JM, Baylac M. 2012. Differences in caste dimorphism among three hornet species (Hymenoptera: Vespidae): forewing size, shape and allometry. *J Evolution Biol* 25:1389-1398.
- Pickett KM, Carpenter JM. 2010. Simultaneous analysis and the origin of eusociality in the Vespidae (Insecta: Hymenoptera). *Arthropod Syst Phylo* 68:3-33.
- Pilgrim EM, Von Dohlen CD, Pitts JP. 2008. Molecular phylogenetics of Vespoidea indicate paraphyly of the superfamily and novel relationships of its component families and subfamilies. *Zool Scr* 37:539-560.
- Ramdaya P, Benton R. 2010. Evolving olfactory systems on the fly. *Trends Genet* 26:307-316.
- Raveret Richter M. 2000. Social wasp (Hymenoptera: Vespidae) Foraging behavior. *Annu Rev Entomol* 45:121-150.
- Rome Q, Muller FJ, Touret-Alby A, Darrouzet E, Perrard A, Villemant C. 2015. Caste differentiation and seasonal changes in *Vespa velutina* (Hym.: Vespidae) colonies in its introduced range. *Journal of Applied Entomology* 139:771-782.
- Roselino AC, Hrcir M, da Cruz Landim C, Giurfa M, Sandoz JC. 2015. Sexual dimorphism and phenotypic plasticity in the antennal lobe of a stingless bee, *Melipona scutellaris*. *J Comp Neurol* 523:1461-1473.
- Rospars JP. 1983. Invariance and sex-specific variations of the glomerular organization in the antennal lobes of a moth, *Mamestra brassicae*, and a butterfly, *Pieris brassicae*. *J Comp Neurol* 220:80-96.
- Rospars JP. 1988. Structure and development of the insect antennodeutocerebral system. *Int J Insect Morphol Embryol* 17:243-294.
- Rospars JP, Chambille I. 1986. Postembryonic growth of the antennal lobes and their identified glomeruli in the cockroach *Blaberus craniifer* burm. (Dictyoptera : Blaberidae): A morphometric study. *Int J Insect Morphol Embryol* 15:393-415.
- Rössler W, Brill M. 2013. Parallel processing in the honeybee olfactory pathway: structure, function, and evolution. *J Comp Physiol A* 199:981-996.
- Rössler W, Zube C. 2011. Dual olfactory pathway in Hymenoptera: evolutionary insights from comparative studies. *Arth StructDev* 40:349-357.
- Ruther J, Sieben S, Schrick B. 1998. Role of cuticular lipids in nestmate recognition of the European hornet *Vespa crabro* L. (Hymenoptera, Vespidae). *Insect Soc* 45:169-179.
- Ruther J, Sieben S, Schrick B. 2002. Nestmate recognition in social wasps: manipulation of hydrocarbon profiles induces aggression in the European hornet. *Naturwissenschaften* 89:111-114.
- Rybak J, Kuss A, Hans L, Zachow S, Hege H-C, Lienhard M, Singer J, Neubert K, Menzel R. 2010. The digital bee brain: integrating and managing neurons in a common 3D reference system. *Front Syst Neurosci* 4:30.
- Sandoz JC. 2006. Odour-evoked responses to queen pheromone components and to plant odours using optical imaging in the antennal lobe of the honey bee drone *Apis mellifera* L. *J Exp Biol* 209:3587-3598.
- Sandoz JC, Galizia CG, Menzel R. 2003. Side-specific olfactory conditioning leads to more specific odor representation between sides but not within sides in the honeybee antennal lobes. *Neuroscience* 120:1137-1148.

- Sharkey MJ, Carpenter JM, Vilhelmsen L, Heraty J, Liljeblad J, Dowling APG, Schulmeister S, Murray D, Deans AR, Ronquist F, Krogmann L, Wheeler WC. 2012. Phylogenetic relationships among superfamilies of Hymenoptera. *Cladistics* 28:80-112.
- Sharma Kavita R, Enzmann Brittany L, Schmidt Y, Moore D, Jones Graeme R, Parker J, Berger Shelley L, Reinberg D, Zwiebel Laurence J, Breit B, Liebig J, Ray A. 2015. Cuticular Hydrocarbon Pheromones for Social Behavior and Their Coding in the Ant Antenna. *Cell Rep* 12:1261-1271.
- Siju KP, Reifenrath A, Scheiblich H, Neupert S, Predel R, Hansson BS, Schachtner J, Ignell R. 2014. Neuropeptides in the antennal lobe of the yellow fever mosquito, *Aedes aegypti*. *J Comp Neurol* 522:592-608.
- Skiri HT, Rø H, Berg BG, Mustaparta H. 2005. Consistent organization of glomeruli in the antennal lobes of related species of heliothine moths. *J Comp Neurol* 491:367-380.
- Smith AR, Seid MA, Jiménez LC, Wcislo WT. 2010. Socially induced brain development in a facultatively eusocial sweat bee *Megalopta genalis* (Halictidae). *Proc R Soc Lond B Biol Sci* 277:2157-2163.
- Spiewok S, Schmolz E, Ruther J. 2006. Mating system of the European hornet *Vespa crabro*: male seeking strategies and evidence for the involvement of a sex pheromone. *J Chem Ecol* 32:2777-2788.
- Spradbery JP. 1973. Wasps. An account of the biology and natural history of social and solitary wasps. University of Washington Press.
- Steinmetz I, Sieben S, Schmolz E. 2002. Chemical trails used for orientation in nest cavities by two vespine wasps, *Vespa crabro* and *Vespula vulgaris*. *Insect Soc* 49:354-356.
- Stieb SM, Kelber C, Wehner R, Rössler W. 2011. Antennal-lobe organization in desert ants of the genus *Cataglyphis*. *Brain Behav Evol* 77: 136-146.
- Strausfeld NJ. 2002. Organization of the honey bee mushroom body: Representation of the calyx within the vertical and gamma lobes. *J Comp Neurol* 450:4-33.
- Strausfeld NJ, Sinakevitch I, Brown SM, Farris SM. 2009. Ground plan of the insect mushroom body: Functional and evolutionary implications. *J Comp Neurol* 513:265-291.
- Streinzer M, Kelber C, Pfabigan S, Kleineidam CJ, Spaethe J. 2013. Sexual dimorphism in the olfactory system of a solitary and a eusocial bee species. *J Comp Neurol* 521:2742-2755.
- Stubblefield JW, Seger J. 1994. Sexual dimorphism in the Hymenoptera. The differences between the sexes: Cambridge University Press.
- Suzuki H. 1975. Antennal movements induced by odour and central projection of the antennal neurones in the honey-bee. *J Insect Physiol* 21:831-847.
- Tan K. 2014. Giant hornet ejecting venom to mark its territory. Abstract, 17th Congress of the IUSSI. <http://hdl.handle.net/2123/11025>.
- Tichy AL, Ray A, Carlson JR. 2008. A new *Drosophila* POU gene, pdm3, acts in odor receptor expression and axon targeting of olfactory neurons. *J Neurosci* 28:7121-7129.
- Vander Meer RK, Breed MD, Espelie KE, Winston ML. 1998. Pheromone communication in social insects. Ants, wasps, bees and termites: Westview, Boulder, CO.
- Veith HJ, Koeniger N, Maschwitz U. 1984. 2-Methyl-3-butene-2-ol, a major component of the alarm pheromone of the hornet *Vespa crabro*. *Naturwissenschaften* 71:328-329.
- Viallanes H. 1887. Etude histologiques et organologiques sur les centres nerveux et les organes des sens des animaux articulés. Quatrième mémoire : Le cerveau de la Guêpe (*Vespa crabro* et *V. vulgaris*). *Ann Sci Nat Zool* 7: 5-100.
- Von Alten, H. 1910. Zur Phylogenie des Hymenopterengehirns. *Jen Zeitschr* 46:513-590.
- Vosshall LB, Wong AM, Axel R. 2000. An olfactory sensory map in the fly brain. *Cell* 102:147-159.

Watanabe H, Nishino H, Nishikawa M, Mizunami M, Yokohari F. 2010. Complete mapping of glomeruli based on sensory nerve branching pattern in the primary olfactory center of the cockroach *Periplaneta americana*. *J Comp Neurol* 518:3907-3930.

Zacharuk RY. 1980. Ultrastructure and Function of Insect Chemosensilla. *Annu Rev Entomology* 25:27-47.

Zube C, Kleineidam CJ, Kirschner S, Neef J, Rössler W. 2008. Organization of the olfactory pathway and odor processing in the antennal lobe of the ant *Camponotus floridanus*. *J Comp Neurol* 506:425-441.

Zube C, Rössler W. 2008. Caste- and sex-specific adaptations within the olfactory pathway in the brain of the ant *Camponotus floridanus*. *Arth Struct Dev* 37:469-479.

Accepted Article

Figure Legends

Figure 1: Wing size in *V. velutina* females. (A) The area between 9 vein intersections on the forewing (yellow polygon) was calculated as a proxy of wing size. (B) Distribution of the wing sizes of all caught *V. velutina* females. Females caught in spring (April – May), at the start of the season, are necessarily founding queens. Females caught in summer-autumn (June to November) are mostly workers. Initially, workers' size is much smaller than queens'. However, workers' wing size increases throughout colony cycle and may eventually (at the end of autumn) overlap with queens'. Therefore, small individuals caught during summer and autumn (dark grey area) and large individuals trapped in spring (light grey area), which could be unambiguously assigned to workers and queens respectively, were used in the experiments.

Figure 2: Head morphology and brain anatomy of the 3 main castes within a *V. velutina* colony. (A, C, E) photographs of *V. velutina* heads (scale bar = 2 mm) showing no noticeable morphological differences between queen (A) and worker heads (C) but a triangular head with longer antennae in males (E). (B, D, F) 3D reconstructions of hornet brains (scale bar = 500 μm). The brains of queen (B) and worker (D) do not show conspicuous differences in their organization but slightly smaller calyces and thinner peduncles were observed in males (F). Heads and brains are shown from the ventral surfaces and are oriented following the same axis. r, rostral; c, caudal. SOG, suboesophageal ganglion; AL, antennal lobe; Me, medulla; Lo lobula; CB, central body; li, lip; co, collar.

Figure 3: Mushroom body morphology in *V. velutina*. (A, B) Frontal optical sections after mass staining in the optic lobe and in the antennal lobe with different fluorescent dyes. (B) Section through the lateral mushroom body calyx (delimited in A, scale bar = 80 μm). The collar receives visual input (magenta) while the lip receives olfactory input (green). (C, D) frontal sections through the brain (scale bar = 400 μm) at respectively 345 μm and 425 μm depths from the ventral surface. (E) Sagittal section of the brain (scale bar = 200 μm). Each brain hemisphere contains a double β lobe pointing dorsally and a single α lobe projecting caudally, with only a fiber tract extending to the ventral surface (black arrowhead). (F) 3D model of a hornet mushroom body, showing the double β lobe and the single α lobe per hemisphere (left mushroom body, scale bar = 200 μm). (E, F) AL, antennal lobe; OL: optic lobe; Me, medulla; Lo lobula; pe: peduncle; ca: calyces; li, lip; co, collar; CB: central body; r, rostral; c, caudal; v: ventral; d: dorsal; m: medial; l: lateral; ri: right; le: left.

Figure 4: (A, B, C) Glomerular volume distribution in the antennal lobe of 6 individuals (dotted lines) of each caste and their respective mean distribution (solid line). Queens (A) and workers (B) exhibit the same glomerular volume distribution. The largest glomeruli were identified at the same locations in the antennal lobes of workers and queens (black dots in B, see also in Fig. 7 and 8D,E). In males (C), the upper part of the distribution extends to much higher volumes than in female castes. The antennal lobe of males contains 7 hypertrophied glomeruli arranged in 2 clusters (MG1-7). Coloring of glomeruli relates to glomerular clusters as in Fig. 7. (D) Relative glomerular volume distribution in the 3 castes and positions of the largest glomeruli with regards to the statistical macroglomerulus threshold (dotted line). Dots indicate the average volume of the 4 (workers and queens) or 7 (males) largest AL glomeruli of each caste. Only males possess glomeruli exceeding the statistical threshold. Bold lines indicate the median of glomerular volumes, boxes the first and the third quartiles (25-75%) and whiskers the 10th to 90th percentiles of the distribution. Scale bar = 100 μ m; MGs: macroglomeruli; r, rostral; c, caudal; m: medial; l: lateral.

Figure 5: Macroglomeruli of the male antennal lobe. (A-D) Confocal images (single section or z projection) at different depths from the ventral surface of a right antennal lobe in a *V. velutina* male (scale bar = 100 μ m). (E-F) Ventral and rostral view, respectively, of a 3 dimensional volume rendering of the male antennal lobe. The macroglomeruli (dotted lines) are arranged in two clusters: the rostral cluster, receiving a thick olfactory tract through the AL, contains 3 macroglomeruli (MG 1-3). The ventro-caudal cluster, located close to the antennal nerve entrance, contains four macroglomeruli (MG 4-7). r, rostral; c, caudal; v: ventral; d: dorsal; m: medial; l: lateral; AN: antennal nerve.

Figure 6: Sensory innervation of the antennal lobe of each caste. (A-O) Projection views of approximately 50 μ m thick slices (~50 optical sections), starting from the ventral surface to the dorsal surface of a right antennal lobe after mass staining of the antennal nerve (scale bar = 100 μ m). The hornet AL contains 9 sensory tracts (T_A - T_I) innervating distinct clusters of glomeruli. All antennal sensory tracts were observed in queens (A, D, G, J, M) workers (B, E, H, K, N) and males (C, F, I, L, O) but some tracts were thicker in males than in females (for instance, T_F in F compared to D and E). r, rostral; c, caudal; m: medial; l: lateral.

Figure 7: 3D reconstructions of the antennal lobes of *V. velutina* female (A, C, E) and male (B, D, F). The 9 clusters of glomeruli and their afferent tracts (T_A - T_I) are color coded and are represented from the ventral to the dorsal surface (right antennal lobe, scale bar = 100 μ m).

Antennal lobe organization is highly similar in males and females but sexually dimorphic clusters that contain macroglomeruli in males are innervated by thicker tracts (T_F and T_G). Dots indicate the four largest glomeruli in females and their homologues in males. Asterisks indicate landmark glomeruli. r, rostral; c, caudal; m: medial; l: lateral.

Figure 8: Efferent innervations of the antennal lobe of *V. velutina*. (A) Projection view of an anterograde mass-fill of all AL output tracts (300 μm thick slice, scale bar = 200 μm). Two prominent tracts (m and l-ALT) project from the AL to the MB calyces and the LH while 3 ml-ALT (arrow heads) projecting broadly to the lateral protocerebrum and the LH. (B, C) Optical section through the AL (B) and MB calyces (C) after differential labeling of the l-ALT (green) and m-ALT (magenta) (scale bars = 100 μm). The two output tracts arborize in segregated parts of the AL, and project differentially to the lips and the basal ring of the MB calyces. (D, E) 3D reconstruction of the *V. velutina* antennal lobe showing the affiliation of glomeruli to the two l-ALT output tracts (D = ventral view and E = dorsal view, scale bar = 100 μm). Glomeruli innervated by the l-ALT (green) are in the rostro-ventral hemilobe of the antennal lobe while m-ALT innervated glomeruli (magenta) are located in the dorso-caudal hemilobe. Two glomeruli (dark blue) show no innervations from ALTs, whereas one glomerulus (yellow) receives processes from both m- and l-ALT. The somata of the l-ALT are spread along the rostral rim of the antennal lobe (ISC) while the somata of the m-ALT are distributed in a caudo-lateral cluster (mSC1) and a rostral cluster (mSC2). (F) Schematic overview of the output network of the antennal lobe. (G) Rostral somata clusters of l-ALT (ISC) and m-ALT neurons (mSC2). Scale bar = 50 μm . (H) Caudo-lateral somata cluster of the l-ALT (m-SC1), Scale bar = 100 μm . All views correspond to the right brain hemisphere.

Figure 9: Morphological similarities between the antennal lobe of *V. velutina* and those of the honeybee and carpenter ants. (A) Dorsal view of a 3 dimensional reconstruction of a *V. velutina* antennal lobe. Compare to Fig 2B-C in Zube et al. (2008) and Fig 4A-C in Kirschner et al. (2006). (B) Projection view of a 30 μm thick slice of a left *V. velutina* antennal lobe after mass staining of the antennal nerve (depth: 175-205 μm). Compare to Fig 1C in Zube et al. (2008) and Fig 3G in Kirschner et al. (2006). (C) Idem as B, but depth: 120-150 μm . Compare to Fig 3E in Kirschner et al. (2006). (D) Ventral view of a 3 dimensional volume rendering of a left female antennal lobe. Compare to Fig 3A in Zube and Rössler (2008) and Fig 2A-F in Nakanishi et al. (2010). For each picture, the antennal nerve orientation was aligned with those of bees and ants as presented in the cited studies. For comparison with previous studies, all images show a left antennal lobe. All scale bars correspond to 100 μm .

Remarkable glomerular clusters and landmark glomeruli are labeled with dotted lines and arrows.

Table 1: Volumes of the *V. velutina* brain neuropils. The absolute volume (in μm^3) and the relative volume (in %) of major brain structures are given for each caste. For multiple structures (ex: collar), the sum of all instances of this structure is given.

Table 2: Cluster characteristics in hornets. Number, volume and output tract affiliation of glomeruli belonging to the nine different clusters of the antennal lobe in female and male hornets.

Table 3: Putative homologies between glomerular clusters in three well-described hymenopteran species. Each line contains corresponding antennal sensory tracts in honeybees (*A. mellifera*), hornets (*V. velutina*) and carpenter ants (*C. floridanus* and *C. japonicus*) with reported numbers of glomeruli and their output tract affiliations. Dark grey cells indicate missing tracts in the given species. Putatively homologous tracts are aligned according to the new denomination implemented in hornets, from most dorsal to most ventral.

^a after Kirschner et al. (2006) and Nishino et al. (2009); ^b after Zube et al. (2008) and Zube and Rössler (2008); ^c after Nakanishi et al. (2010).

Table 4: Typical features of glomerular clusters across species. Each line gives the relative depth, the localization and the output tract affiliation of each cluster. The fourth column indicates the projection pattern (orientation) of the olfactory sensory tract. The fifth and the sixth columns specify typical glomerular features such as relative sizes, shapes and OSN innervation types (in the whole glomerulus or only in the glomerular cortex).

Competing interest

All authors have confirmed that there is no identified conflict of interest including any financial, personal or other relationships with other people or organizations within 3 years of beginning the submitted work that can inappropriately influence, or be perceived to influence, their work.

Authors' contributions

All authors had full access to all the data in the study and take responsibility for the integrity of the data and the accuracy of the data analysis. Study concept and design: AC, DT and JCS.

Acquisition of data: AC with help from BL. Analysis and interpretation of data: AC, JCS.

Drafting of the manuscript: AC, JCS. Critical revision of the manuscript for important intellectual content: AC, DT, JCS. Obtained funding: JCS, Study supervision: JCS.

Accepted Article

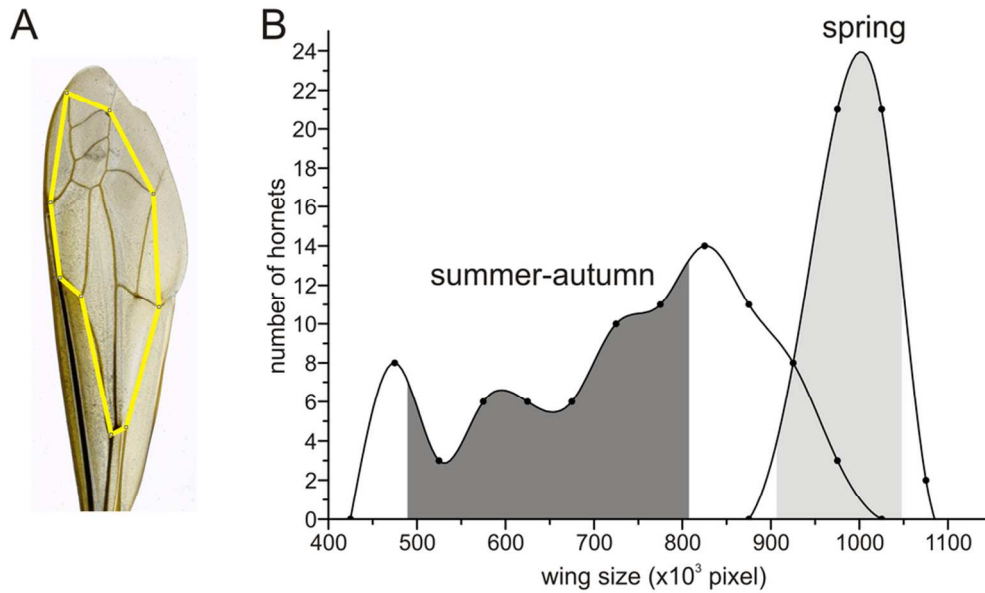


Figure 1: Wing size in *V. velutina* females. (A) The area between 9 vein intersections on the forewing (yellow polygon) was calculated as a proxy of wing size. (B) Distribution of the wing sizes of all caught *V. velutina* females. Females caught in spring (April – May), at the start of the season, are necessarily founding queens. Females caught in summer-autumn (June to November) are mostly workers. Initially, workers' size is much smaller than queens'. However, workers' wing size increases throughout colony cycle and may eventually (at the end of autumn) overlap with queens'. Therefore, small individuals caught during summer and autumn (dark grey area) and large individuals trapped in spring (light grey area), which could be unambiguously assigned to workers and queens respectively, were used in the experiments.

87x51mm (300 x 300 DPI)

Accept

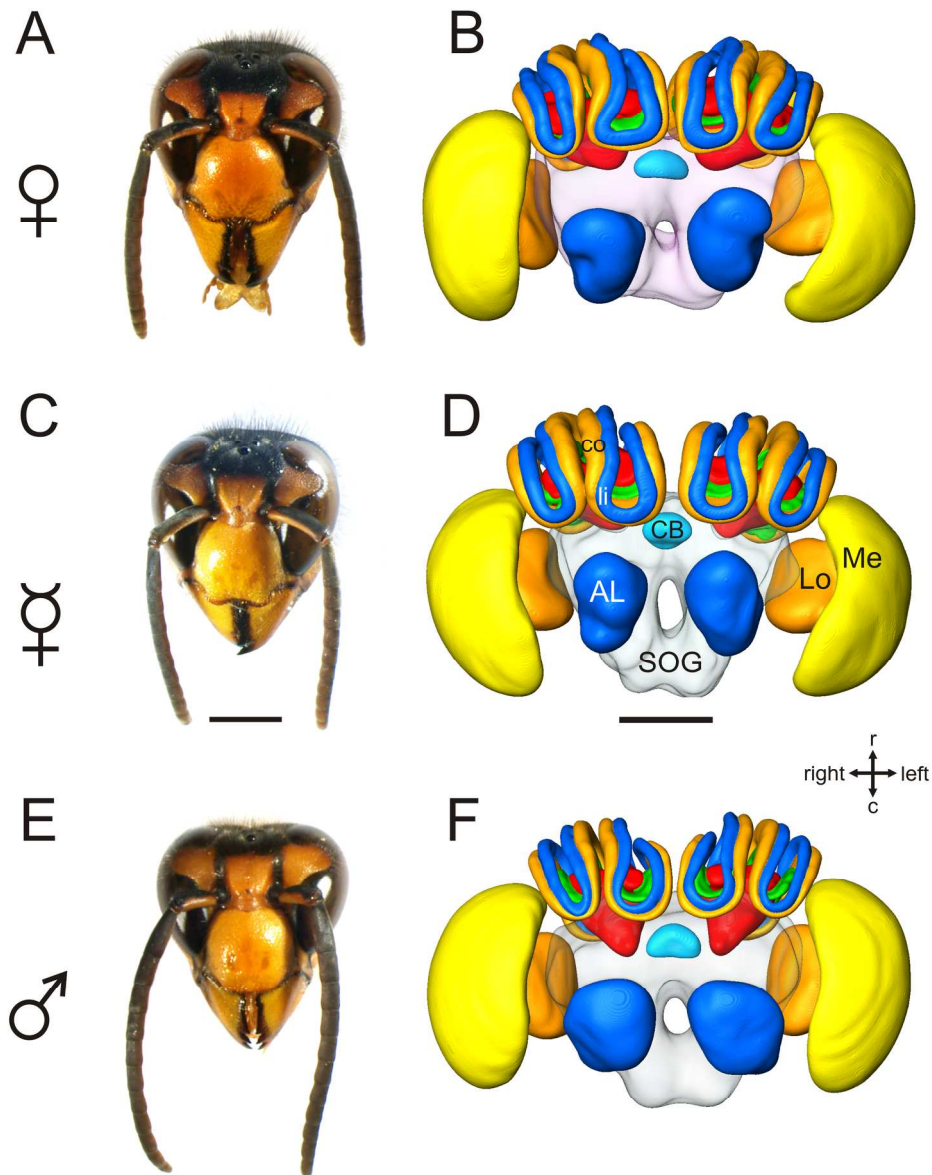


Figure 2: Head morphology and brain anatomy of the 3 main castes within a *V. velutina* colony. (A, C, E) photographs of *V. velutina* heads (scale bar = 2 mm) showing no noticeable morphological differences between queen (A) and worker heads (C) but a triangular head with longer antennae in males (E). (B, D, F) 3D reconstructions of hornet brains (scale bar = 500 μ m). The brains of queen (B) and worker (D) do not show conspicuous differences in their organization but slightly smaller calyces and thinner peduncles were observed in males (F). Heads and brains are shown from the ventral surfaces and are oriented following the same axis. r, rostral; c, caudal. SOG, subesophageal ganglion; AL, antennal lobe; Me, medulla; Lo lobula; CB, central body; li, lip; co, collar.
173x221mm (300 x 300 DPI)

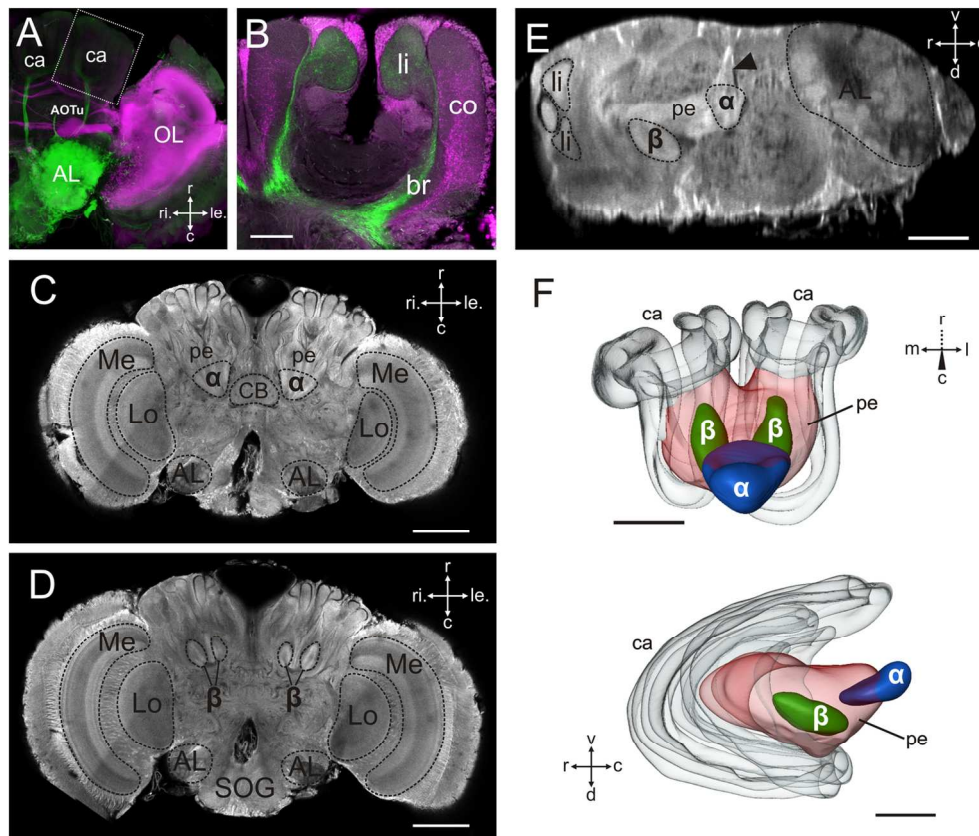


Figure 3: Mushroom body morphology in *V. velutina*. (A, B) Frontal optical sections after mass staining in the optic lobe and in the antennal lobe with different fluorescent dyes. (B) Section through the lateral mushroom body calyx (delimited in A, scale bar = 80 μm). The collar receives visual input (magenta) while the lip receives olfactory input (green). (C, D) Frontal sections through the brain (scale bar = 400 μm) at respectively 345 μm and 425 μm depths from the ventral surface. (E) Sagittal section of the brain (scale bar = 200 μm). Each brain hemisphere contains a double β lobe pointing dorsally and a single α lobe projecting caudally, with only a fiber tract extending to the ventral surface (black arrowhead). (F) 3D model of a hornet mushroom body, showing the double β lobe and the single α lobe per hemisphere (left mushroom body, scale bar = 200 μm). (E, F) AL, antennal lobe; OL: optic lobe; Me, medulla; Lo lobula; pe: peduncle; ca: calyces; li, lip; co, collar; CB: central body; r, rostral; c, caudal; v: ventral; d: dorsal; m: medial; l: lateral; ri: right; le: left.

137x116mm (300 x 300 DPI)

Acc

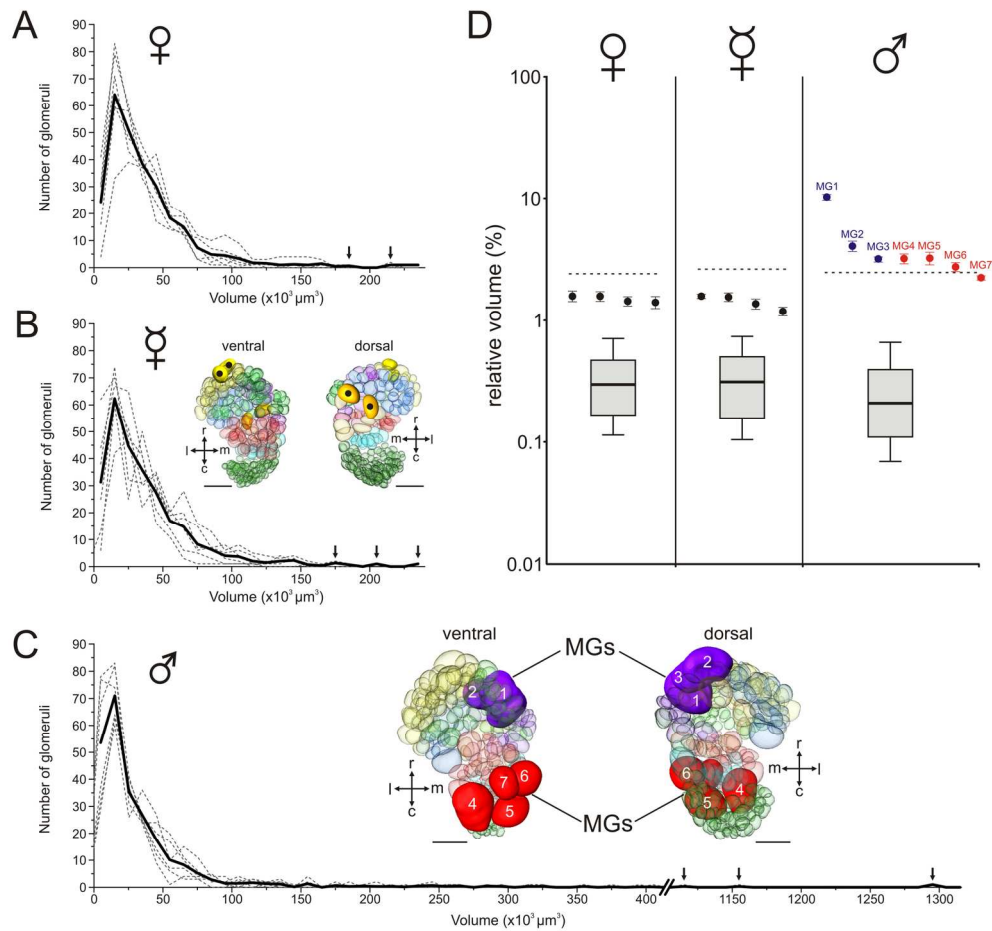


Figure 4: (A, B, C) Glomerular volume distribution in the antennal lobe of 6 individuals (dotted lines) of each caste and their respective mean distribution (solid line). Queens (A) and workers (B) exhibit the same glomerular volume distribution. The largest glomeruli were identified at the same locations in the antennal lobes of workers and queens (black dots in B, see also in Fig. 7 and 8D,E). In males (C), the upper part of the distribution extends to much higher volumes than in female castes. The antennal lobe of males contains 7 hypertrophied glomeruli arranged in 2 clusters (MG1-7). Coloring of glomeruli relates to glomerular clusters as in Fig. 7. (D) Relative glomerular volume distribution in the 3 castes and positions of the largest glomeruli with regards to the statistical macroglomerulus threshold (dotted line). Dots indicate the average volume of the 4 (workers and queens) or 7 (males) largest AL glomeruli of each caste. Only males possess glomeruli exceeding the statistical threshold. Bold lines indicate the median of glomerular volumes, boxes the first and the third quartiles (25-75%) and whiskers the 10th to 90th percentiles of the distribution. Scale bar = 100 μm ; MGs: macroglomeruli; r, rostral; c, caudal; m: medial; l: lateral. 166x156mm (300 x 300 DPI)

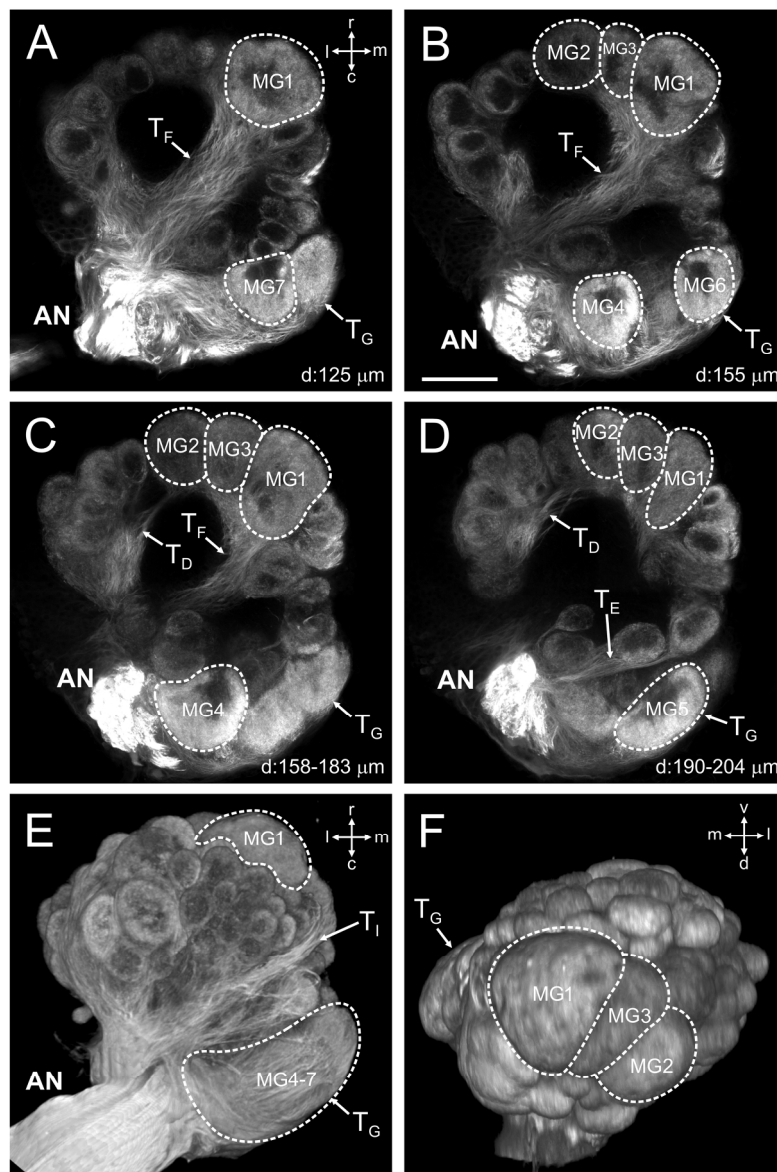


Figure 5: Macroglomeruli of the male antennal lobe. (A-D) Confocal images (single section or z projection) at different depths from the ventral surface of a right antennal lobe in a *V. velutina* male (scale bar = 100 μm). (E-F) Ventral and rostral view, respectively, of a 3 dimensional volume rendering of the male antennal lobe.

The macroglomeruli (dotted lines) are arranged in two clusters: the rostral cluster, receiving a thick olfactory tract through the AL, contains 3 macroglomeruli (MG 1-3). The ventro-caudal cluster, located close to the antennal nerve entrance, contains four macroglomeruli (MG 4-7). r, rostral; c, caudal; v, ventral; d: dorsal; m: medial; l: lateral; AN: antennal nerve.

161x240mm (300 x 300 DPI)

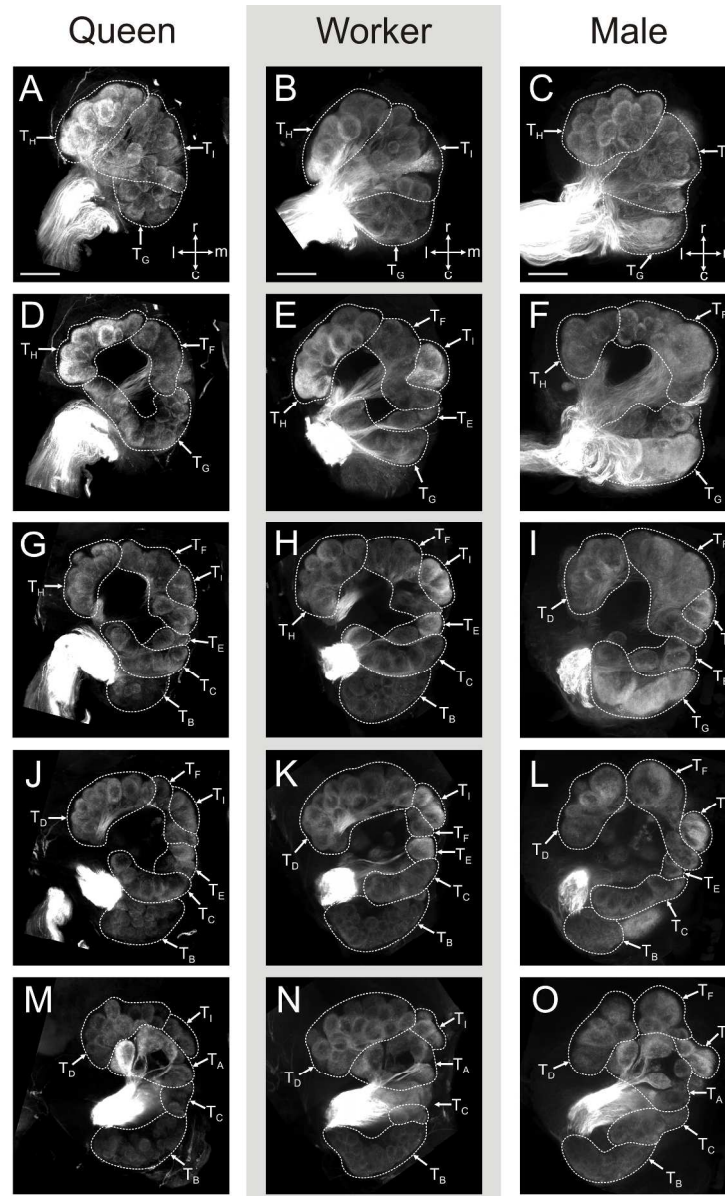


Figure 6: Sensory innervation of the antennal lobe of each caste. (A-O) Projection views of approximately 50 μm thick slices (~ 50 optical sections), starting from the ventral surface to the dorsal surface of a right antennal lobe after mass staining of the antennal nerve (scale bar = 100 μm). The hornet AL contains 9 sensory tracts (TA-TI) innervating distinct clusters of glomeruli. All antennal sensory tracts were observed in queens (A, D, G, J, M) workers (B, E, H, K, N) and males (C, F, I, L, O) but some tracts were thicker in males than in females (for instance, TF in F compared to D and E). r, rostral; c, caudal; m: medial; l: lateral.

210x338mm (300 x 300 DPI)

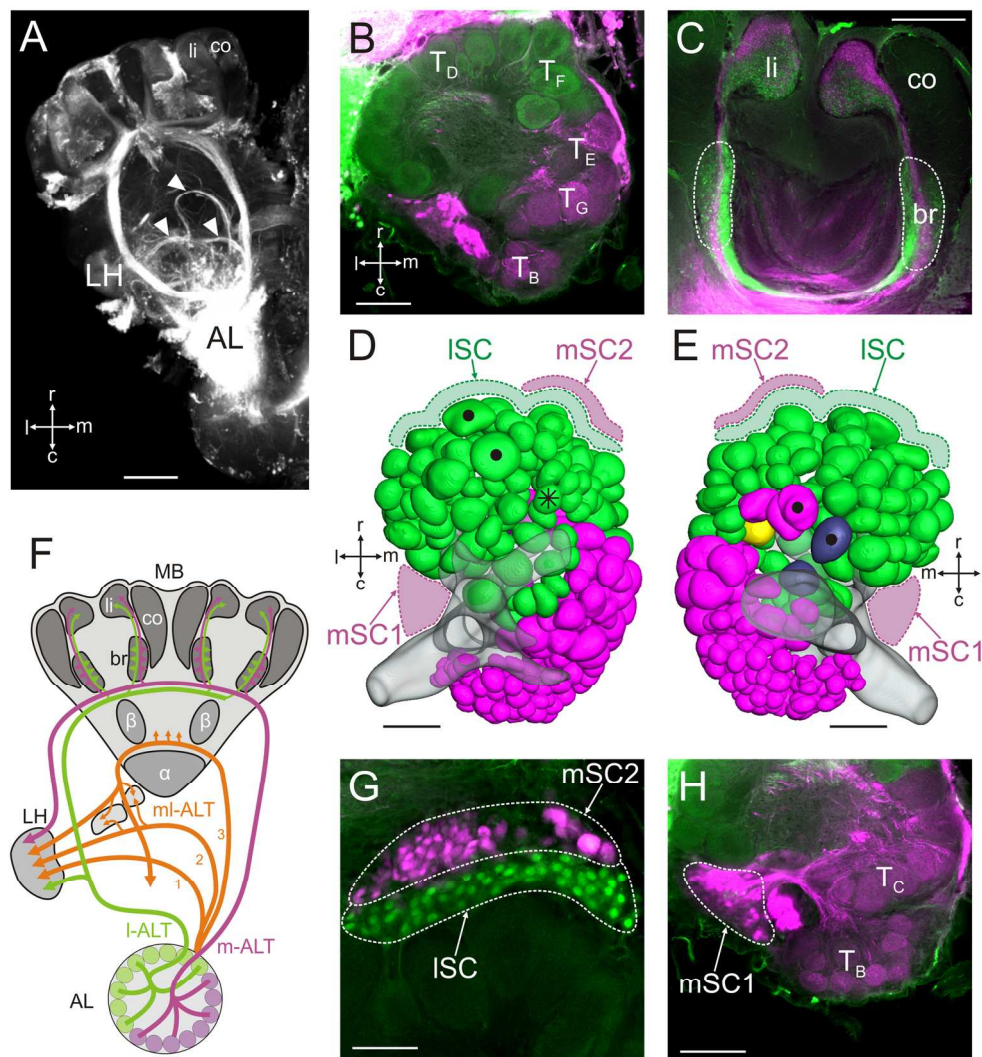


Figure 8: Efferent innervations of the antennal lobe of *V. velutina*. (A) Projection view of an anterograde mass-fill of all AL output tracts (300 μm thick slice, scale bar = 200 μm). Two prominent tracts (m and I-ALT) project from the AL to the MB calyces and the LH while 3 ml-ALT (arrow heads) projecting broadly to the lateral protocerebrum and the LH. (B, C) Optical section through the AL (B) and MB calyces (C) after differential labeling of the I-ALT (green) and m-ALT (magenta) (scale bars = 100 μm). The two output tracts arborize in segregated parts of the AL, and project differentially to the lips and the basal ring of the MB calyces. (D, E) 3D reconstruction of the *V. velutina* antennal lobe showing the affiliation of glomeruli to the two I-ALT output tracts (D = ventral view and E = dorsal view, scale bar = 100 μm). Glomeruli innervated by the I-ALT (green) are in the rostro-ventral hemilobe of the antennal lobe while m-ALT innervated glomeruli (magenta) are located in the dorso-caudal hemilobe. Two glomeruli (dark blue) show no innervations from ALTs, whereas one glomerulus (yellow) receives processes from both m- and I-ALT. The somata of the I-ALT are spread along the rostral rim of the antennal lobe (ISC) while the somata of the m-ALT are distributed in a caudo-lateral cluster (mSC1) and a rostral cluster (mSC2). (F) Schematic overview of the output network of the antennal lobe. (G) Rostral somata clusters of I-ALT (ISC) and m-ALT neurons (mSC2). Scale bar = 50 μm . (H) Caudo-lateral somata cluster of the I-ALT (m-SC1), Scale bar = 100 μm . All views correspond to the right brain hemisphere.
162x175mm (300 x 300 DPI)

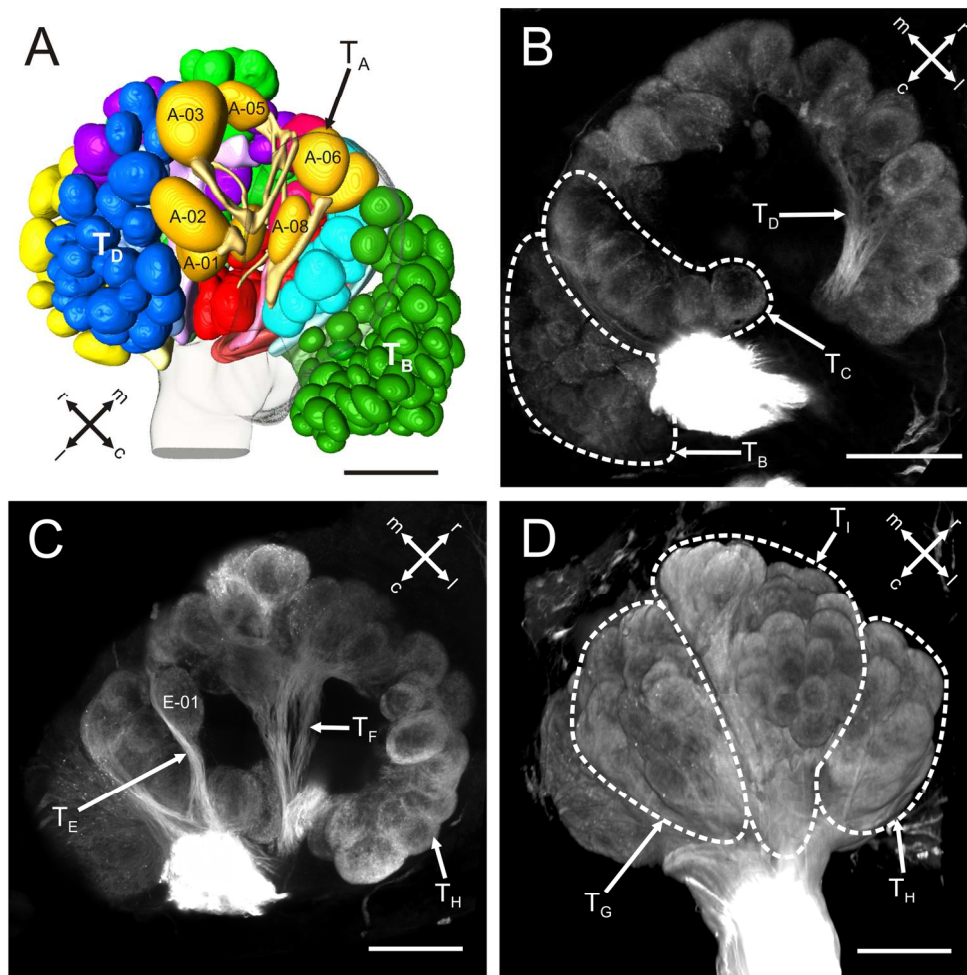


Figure 9: Morphological similarities between the antennal lobe of *V. velutina* and those of the honeybee and carpenter ants. (A) Dorsal view of a 3 dimensional reconstruction of a *V. velutina* antennal lobe. Compare to Fig 2B-C in Zube et al. (2008) and Fig 4A-C in Kirschner et al. (2006). (B) Projection view of a 30 μm thick slice of a left *V. velutina* antennal lobe after mass staining of the antennal nerve (depth: 175-205 μm). Compare to Fig 1C in Zube et al. (2008) and Fig 3G in Kirschner et al. (2006). (C) Idem as B, but depth: 120-150 μm . Compare to Fig 3E in Kirschner et al. (2006). (D) Ventral view of a 3 dimensional volume rendering of a left female antennal lobe. Compare to Fig 3A in Zube and Rössler (2008) and Fig 2A-F in Nakanishi et al. (2010). For each picture, the antennal nerve orientation was aligned with those of bees and ants as presented in the cited studies. For comparison with previous studies, all images show a left antennal lobe. All scale bars correspond to 100 μm . Remarkable glomerular clusters and landmark glomeruli are labeled with dotted lines and arrows.

159x158mm (300 x 300 DPI)

Table 1: Volumes of the *V. velutina* brain neuropils.

The absolute volume (in μm^3) and the relative volume (in %) of major brain structures are given for each caste. For multiple structures (ex: collar), the sum of all instances of this structure is given.

		Protocerebrum	Medulla	Lobula	Antennal lobe	Collar	Lip	Basal ring	Peduncle	Central body	total
queen	$\times 10^6 \mu\text{m}^3$	522.03	292.71	103.88	92.63	86.18	59.55	23.49	109.64	3.36	1293.48
	%	40.36	22.63	8.03	7.16	6.66	4.60	1.82	8.48	0.26	100
worker	$\times 10^6 \mu\text{m}^3$	442.80	291.68	92.16	84.08	109.15	55.12	22.20	85.85	3.76	1186.82
	%	37.31	24.58	7.77	7.08	9.20	4.64	1.87	7.23	0.32	100
male	$\times 10^6 \mu\text{m}^3$	428.01	273.23	94.85	97.46	58.73	30.83	15.98	58.17	3.43	1060.70
	%	40.35	25.76	8.94	9.19	5.54	2.91	1.51	5.48	0.32	100

Table 2: Cluster characteristics in hornets

Number, volume and output tract affiliation of glomeruli belonging to the nine different clusters of the antennal lobe in female and male hornets.

	T _A	T _B	T _C	T _D	T _E	T _F	T _G	T _H	T _I	Σ
Σ glomeruli	8	90	15	29	3	22	33	29	37	266
Min volume (x10 ³ μm ³)	51.3	3.3	11.3	10.5	58.9	4.6	8.1	2.5	10.3	
Max volume (x10 ³ μm ³)	200.1	31.2	57.7	92.3	85.5	74.6	66.2	104.5	103.6	
Mean volume (x10 ³ μm ³)	91.1	12.6	33.0	35.7	72.8	35.4	33.5	37.6	32.1	
output tract	m-ALT (6 out of 8)	m-ALT	m-ALT	I-ALT	m-ALT (2) / both-ALT (1)	I-ALT	I-ALT (9) / m-ALT (24)	I-ALT	I-ALT	m-ALT (138) / I-ALT (127)
Σ glomeruli	8	74	17	24	3	21	32	32	38	249
Min volume (x10 ³ μm ³)	39.4	2.2	8.5	6.9	13.7	1.2	3.72	5.3	4.1	
Max volume (x10 ³ μm ³)	136.1	25.2	47.4	250.7	38.4	763.1	285.6	87.3	62.9	
Mean volume (x10 ³ μm ³)	67.1	8.9	21.8	44.1	25.8	90.9	51.3	30.8	22.7	

Table 3: Putative homologies between glomerular clusters in three well-described hymenopteran species

Each line contains corresponding antennal sensory tracts in honeybees (*A. mellifera*), hornets (*V. velutina*) and carpenter ants (*C. floridanus* and *C. japonicus*) with reported numbers of glomeruli and their output tract affiliations. Dark grey cells indicate missing tracts in the given species. Putatively homologous tracts are aligned according to the new denomination implemented in hornets, from most dorsal to most ventral.

<i>A. mellifera</i> ^a			<i>V. velutina</i>			<i>C. floridanus</i> ^b and <i>C. japonicus</i> ^c		
input tracts	∑ glomeruli	output tracts	input tracts	∑ glomeruli	output tracts	input tracts	∑ glomeruli	output tracts
T4	7	m-ALT / 5 out of 7	T _A	8	m-ALT / 6 out of 8	T7	6 or 10	m-ALT / 5 out of 6
T3b	12	m-ALT	T _B	90	m-ALT	T6	128 or 140	m-ALT
T3c	42	m-ALT	T _C	15	m-ALT	T5	36 or 35	m-ALT
			T _D	30	I-ALT	T4	78 or 95	I-ALT
T2	7	I-ALT / m-ALT / both	T _E	3	m-ALT / both			
T1	72	I-ALT	T _F	20	I-ALT			
T3a	24	I-ALT / m-ALT	T _G	30	I-ALT / m-ALT	T3	96 or 110	I-ALT / m-ALT
			T _H	30	I-ALT	T2	56 or 45	I-ALT
			T _I	40	I-ALT	T1	34 or 35	I-ALT

^a after Kirschner et al. (2006) and Nishino et al. (2009)

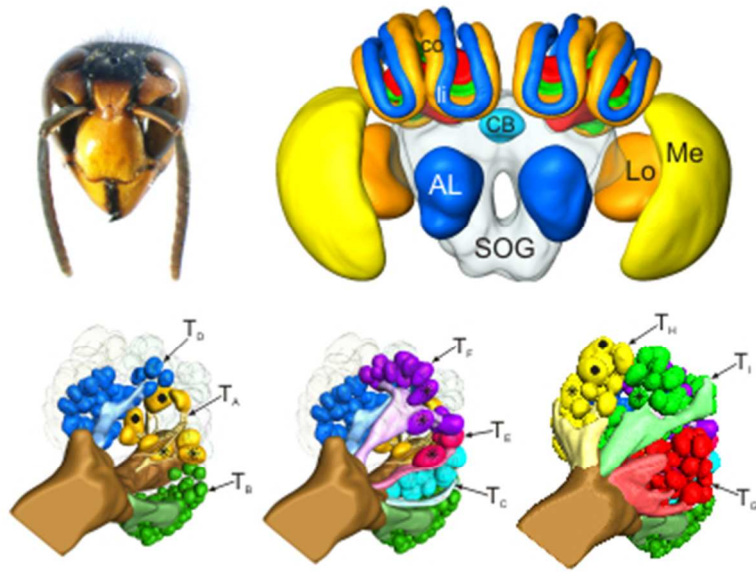
^b after Zube et al. (2008) and Zube and Rössler (2008)

^c after Nakanishi et al. (2010)

Table 4: Typical features of glomerular clusters across species

Each line gives the relative depth, the localization and the output tract affiliation of each cluster. The fourth column indicates the projection pattern (orientation) of the olfactory sensory tract. The fifth and the sixth columns specify typical glomerular features such as relative sizes, shapes and OSN innervation types (in the whole glomerulus or only in the glomerular cortex).

	Depth	Cluster position	Uniglomerular PN output	OSN input pattern	Relative glomerular size	Glomerular features / OSN innervation
T _A	dorsal	necklace arrangement	m-ALT / none	several bundles	large	egg-shaped, dense innervation in both core and cortex
T _B	dorsal	caudal/medial	m-ALT	from caudo-ventral surface	small	clumped glomeruli, innervation in cortex
T _C	relatively dorsal	caudal/medial	m-ALT	from caudal to medial (running along TB)	normal	innervation in cortex thin cortex
T _D	relatively dorsal	rostral/lateral	I-ALT	thick, inner lateral part of the AL	normal	innervation in cortex
T _E	medium	medial	I-ALT / m-ALT / both	through the inner medial part of the AL	relatively large	dense innervation in both core and cortex
T _F	medium	rostral	I-ALT	transversally through AL midline	normal (possible sex dimorphism)	innervation in cortex
T _G	relatively ventral	medial	I-ALT / m-ALT	from caudal periphery to medial	normal (possible sex dimorphism)	innervation in cortex
T _H	ventral	lateral	I-ALT	From lateral periphery to rostral	relatively large	innervation in cortex
T _I	ventral	rostral	I-ALT	caudal to rostral	normal	innervation in cortex



141x105mm (72 x 72 DPI)

Accepted

Graphical abstract text

Using neural tracers and confocal microscopy, the authors analyze the morphology of the hornet *Vespa velutina* brain, especially its antennal lobe, and show a low polymorphism between castes and sexes. Introducing a novel nomenclature for glomerular clusters, they propose homologies with the antennal lobes of ants and bees.

Accepted Article

